A REMEDIAL APPROACH TO REDUCE RESIDUAL HEAT LEFT BEHIND BY SHUTDOWN AQUIFER THERMAL ENERGY STORAGE SYSTEMS: A NUMERICAL MODELING STUDY

A Thesis

by

MATTHEW ROSEBOOM

Submitted to the Graduate and Professional School of
Texas A&M University
in partial fulfillment of the requirements for the degree of

MASTER OF SCIENCE

Chair of Committee,	Hongbin Zhan
Committee Members,	Yuefeng Sun
	Itza Mendoza-Sanchez
Head of Department,	Julie Newman

May 2023

Major Subject: Geophysics

ABSTRACT

Utilizing aquifer thermal energy storage and recovery systems (ATES) and groundwater heat pumps (GWHP) for seasonal space heating and cooling in public and commercial spaces is one solution to reduce fossil fuel consumption for energy and heat production. ATES applications are a form of thermal energy storage that integrates an open or closed-loop well system in groundwater aquifers where warm and cold-water are injected and extracted for heating and cooling purposes in residential and public spaces depending on energy demand. Since this is a low-enthalpy system utilizing shallow groundwater aquifers, temperatures for this study are limited to a range of 5°C-30°C based upon previous environmental work. From an environmental standpoint there are limited studies that assess methods for reducing thermal energy stored in groundwater aquifers to achieve pre-ATES deployment conditions as it is important to understand subsurface conditions once these systems are not in use anymore.

This research aims to take a remedial approach by developing numerical models for simulating long-term transient temperature distributions in porous media after the shutdown of a pre-existing ATES system for 30 years. Additionally, it serves to investigate the most effective method to reduce thermal energy stored in an aquifer through cold-water injection push-pull testing to bring the aquifer back to steady-state equilibrium conditions where the temperature remains within 5°C of the initial ambient groundwater temperature (uncertainty is due to changes in surface temperatures over time). Results from evaluating the long-term effect of the shutdown ATES system after five years of operation indicate that thermal energy stored near the warm-well decreases at a faster rate within the first 10 years after the shutdown and proceed to gradually slow as temperatures between wells approach within 2°C to 3°C above pre-ATES

deployment conditions. Findings from cold-water injection indicate that the aquifer can be remediated within 5-years given flowrates of 200-300 m^3/d to reduced temperature distributions to below 1°C above pre-ATES deployment conditions, ensuring the longevity and health of the aquifer.

DEDICATION

To my mother, father, and brother.

ACKNOWLEDGEMENTS

Firstly, I would like to give many thanks to my advisor, Dr. Zhan, who has been nothing but encouraging and supportive through the course of this research and during my studies. He has given me the guidance and foundation of what it means to be a successful young researcher and offered his recommendation in my ideas and aspirations.

I would like to thank my committee members, Dr. Sun, and Dr. Mendoza, for their support in my research and for their dedicated time.

It has been a pleasure to work alongside and to be a part of a great group of friends, colleagues, faculty, and especially the staff within the Geology and Geophysics department. Thank you for all the memories, help, and support and for making my time at Texas A&M University a wonderful experience.

Finally, I would not be going through these steps in my life without the encouragement, patience, and love from my family. Thank you.

CONTRIBUTORS AND FUNDING SOURCES

Contributors

This work was supervised by a thesis committee consisting of Professor Hongbin Zhan and Professor Yuefeng Sun of the Department of Geology and Geophysics, and Professor Itza Mendoza-Sanchez of the Department of Environmental & Occupational Health.

Funding Sources

Graduate study was supported by fellowships from Texas A&M University, namely, the Wayne M. Ahr ’65 Endowed Memorial Fellowship and the Leonard Gage Larsen Memorial Fellowship.

NOMENCLATURE

ATES	Aquifer Thermal Energy Storage
CFD	Central Finite Difference
FDM	Finite Difference Method
FEM	Finite Element Method
GWHP	Groundwater Heat Pump
J	Joule; energy
K	Kelvin; temperature
L	Length
M	Mass
m	Meters; length
MOC	Method of Characteristics
MT3DMS	Modular 3-Dimensional Transport Multi-Species
T	Time
TVD	Total Variable Diminishing
USGS	United States Geological Survey
W	Watts; power

TABLE OF CONTENTS

Page

LIST OF FIGURES

Page

LIST OF TABLES

Page

1. INTRODUCTION

1.1 Objectives

Understanding the effects that ATES systems have on the subsurface has been a principal area of research concerning the longevity and sustainability of thermal energy storage, but there are limited studies performed that enable our understanding of the long-term thermal impact on an aquifer after an ATES system has been shut down. It is crucial to understand how thermal energy stored in the subsurface can be dissipated or reduced to bring the aquifer conditions back to equilibrium, as heat storage can last more than 10,000 years in certain hydrogeological conditions. The effort of this research aims to build on our understanding of heat transport in groundwater aquifers while delivering modeling scenarios that simulate potential solutions for limiting or reducing heat flow in the subsurface over a duration of 25 years. Previous studies regarding numerical model analyses of thermal dispersion shared with the effects of cold-water injection into the aquifer have been limited to outlooks of 15-to-20-year periods. Cold-water injection into the preconditioned warm aquifer is a significant part of the puzzle when identifying strategies to minimize the spread of heat flow to the surroundings. In the case where one may want to utilize the same aquifer after ATES operations has ceased (i.e., for other public or commercial purposes related to drinking water, irrigation, etc.), knowledge of how well an aquifer will respond to cold-water injection and push-pull testing over an extended period is crucial.

The extent of this work intends to determine appropriate modeling approaches that simulate an aquifer's thermal response to cold-water injection and push-pull testing to develop the aquifer back to equilibrium where the groundwater temperature falls within 5°C of initial

steady state conditions. It is known that increased groundwater temperatures can potentially place a burden on water quality, where increased microbial activity, chemical mixing due to injection and extraction, and reduced mechanical properties of the porous media all contribute to the health of the aquifer. The focus here is given as an ATES system that is developed for a shallow (50m depth) and low enthalpy confined groundwater system in which injection temperatures do not exceed 25°C. ATES system deployment and research and development framework have a 50-year history, and there are currently more than 2,800 systems in operation globally. Out of all these systems 99% are low temperature with storage temperatures of <25°C, most of which (85%) are in the Netherlands, and the remaining (10%) are in Sweden, Denmark, Belgium, U.S., China, and Japan (Fleuchaus, 2020). Though these low-enthalpy systems are not likely to cause negative effects on the hydrogeologic subsurface, it should remain a concern when one is evaluating the long-term health of groundwater aquifers.

The leading hypothesis is, in simulating scenarios of cold-water injection and push-pull testing using preconditioned groundwater, thermal dispersion in the groundwater aquifer will be reduced largely near the borehole injection/extraction regions and residual heat further away from the borehole while still within the well capture zone, will be reduced back to within 5°C of equilibrium conditions. Residual heat will remain dispersed in the aquifer outside the capture zone as well as near the confining layer boundaries due to the potential for heat stored in the confining clay layers to bleed out into the aquifer over time.

The effect of thermal energy stored in porous media after the shutdown of an ATES system is currently not well known, even though increased groundwater temperatures may have some degree of impact on drinking water quality due to changes in physical, chemical, and microbial processes. The proposed work is significant because it is a critical step towards

ensuring the feasibility and environmental sustainability of thermal energy storage systems which will help contribute to our global energy transition from fossil fuels to renewable and clean energy technologies that utilize Earth's subsurface. This work will 1) offer a stronger understanding of heat transport in confined groundwater aquifers generated by ATES systems 2) provide new knowledge on ways thermal energy can be reduced in porous media without leaving conditions to develop naturally for much longer periods of time and 3) improve the overall outlook for implementing these clean energy solutions on a larger-scale where they can significantly contribute to the heating and cooling of public buildings in more densely populated environments.

1.2 Review of Relevant Literature

The three-dimensional (3D) coupled thermo-hydrogeological conceptual model, designed for a shallow confined aquifer thermal energy storage system in porous media that is bounded by upper and lower clay layers, should consider all heat transport processes. The conceptual model assumptions are: an aquifer of having no groundwater flow in the longitudinal and lateral directions, that is homogeneous and anisotropic, and no thermal gradient is applied between the porous media and confining layers. Though there have been studies comparing numerical codes applied to thermos-hydrogeological process, such as MT3DMS (Modular 3-Dimensional Transport Multi-Species) with analytical solutions for investigating thermal dispersion in porous media, there are limited investigations that aim to account for heat transfer of all modes during thermal injection. Stopa and Wojnarowski (2006) developed an analytical solution using the method of characteristics (MOC), to study the thermal front velocity during cold-water injection into the low-enthalpy groundwater aquifer. They considered the heat capacity and density of the material and fluid in porous media to be dependent on temperature and neglected the longitudinal

heat conduction of the system. Other semi-analytical solutions developed by Yang and Yeh (2008), and Li et al. (2010) used the Laplace transform to predict temperature distributions in an ATES system for a confined aquifer but neglected vertical flow and thermal conduction perpendicular to the aquifer. A semi-analytical solution for transient heat transfer in porous media due to thermal injection which includes advection, conduction, and heat loss from the geothermal aquifer to confining layers was developed by Li et al. (2010).

Additionally, there are limited studies that address thermal remediation methods of aquifers utilized for thermal energy storage systems. Various numerical investigations have simulated the long-term effects of ATES cyclic mode operations given different injection and pumping rates and injection temperatures below 25°C, though there are no found studies that aim to evaluate the shutdown and thermal remediation of the groundwater aquifer by single-well cold-water injection and extraction scenarios. Lee (2008) conducted a numerical investigation that studied the effects of various ATES operating conditions and aquifer characteristics on thermal recoveries for a 10-year continuous injection and production period, though injection temperatures were maintained at 5°C on the cold side and 25°C on the warm side with no indication of reducing the average aquifer temperature back to equilibrium conditions (natural ambient groundwater temperatures). In recent years, the concept of combining ATES with subsurface remediation, specifically looking at the relation between temperature increase and biodegradation rates has been studied. Meng et al. (2021), published a study that aimed to numerically investigate the impacts of periodic high-temperature heat storage (70°C) through ATES on the fate and transport of chlorinated hydrocarbon contaminants (i.e., TCE) in a shallow unconfined aquifer for a 5-year period. Though Meng's study implies remedial methods for reducing a contaminant plume using ATES technology, there is still the need for field and

numerical investigations that aim to dissipate and reduce the residual thermal energy stored in porous media after ATES operations are shut down for a period of 25+ years.

2. CONCEPTUAL OVERVIEW

Conceptually, illustrated in Figures 2.1 and 2.2, the model represents an open-loop ATES systems with five-years of operation and will replicate an existing shallow-depth, low-enthalpy, open-loop ATES system following ideal hydrogeologic conditions and site suitability for optimal thermal energy storage and recovery. The thermophysical rock and fluid properties of the aquifer and confining rock layers are provided in Table 2.1 of Appendix A. The represented aquifer is configured as a homogeneous, anisotropic, three-layer system comprised of upper and lower confining clay layers with equivalent physical, fluid, and thermal properties and the aquifer layer consisting of unconsolidated alluvial fine sandstone. Anisotropy is given by the variation in horizontal and vertical hydraulic and thermal conductivities. There is no ambient groundwater flow, and this is represented with fixed hydraulic head values of 100 m at the left and right boundaries.

The hypothesis of this study is that cyclic injection and extraction of warm and cold-water in a low ambient groundwater flow aquifer will create two separate regions of temperature anomalies, where cooler groundwater will remain proximal to the cold-water injection/extraction well and warmer groundwater will remain proximal to the warm-water injection/extraction well. There will be minimal effect of thermal interference between the two wells (half the lateral

distance) as the distance between the wells will be large enough so that the thermal front from the warm injection well will not propagate to more than half the distance to the cold well.

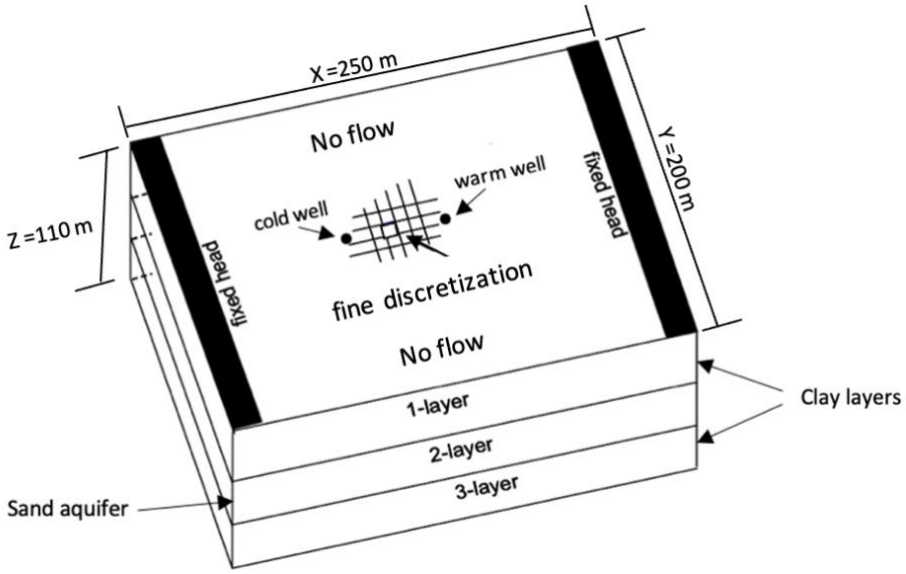

Figure 2.1 3D conceptual model domain (Labels modified from Hecht-Méndez, et al. 2009).

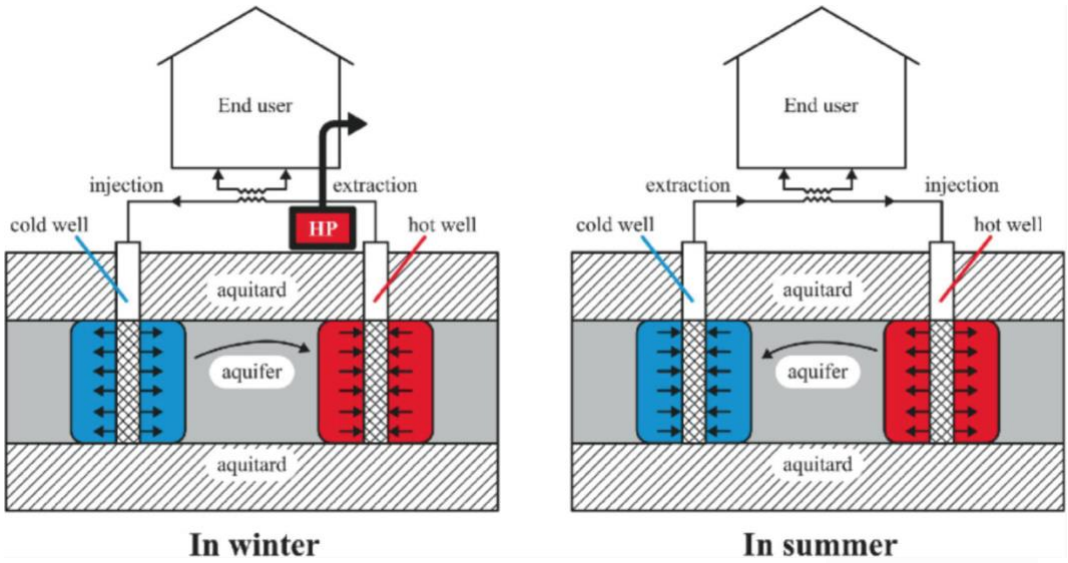

Figure 2.2 Schematic of ATES system for cyclic operations (Ocłoń P. 2021).

The second case addresses the problem of long-term thermal dispersion and diffusion in the aquifer through simulating transient heat distributions once the ATES system has been shut down, referred to as the "idle" period. This model will utilize the preconditioned ATES system developed in chapter one where the initial temperatures in the formation layers are representative of the thermal energy stored at t = 5 years. The "idle" period deals with both warm and cold wells having zero flowrate conditions for the next 30 years, simulated. The results of this model will form the base case scenario for evaluating how heat is dispersed in porous media and diffused through the confining layers over 1, 5, 10, 15, and 30-years. The idle period will provide the transient temperature distribution profiles across the aquifer and will further be used to compare against the thermal distribution profiles generated by the push-pull testing scenarios. The hypothesis of this study infers that warmer temperature distributions will form radially outward away from the warm well with decreasing temperatures at distance from the well. Cooler temperature distributions will resemble the temperatures of the ambient groundwater flow and will also form radially outward from the cold well with minimal changes in temperature away from the well. The temperature distribution halfway between the two wells will have slightly warmer temperatures than that of the ambient groundwater flow.

The third case focuses on the remedial approach for reducing the thermal energy stored in the aquifer by simulating cold-water well injection and groundwater extraction through a series of push-pull testing. Simulating various cases of push-pull tests is a method that can aid in the understanding of how an aquifer may return to equilibrium conditions (groundwater flow and temperature conditions before the ATES system was implemented) by engineered systems. To reduce the amount of thermal energy stored near the warm well region a series of cold-water injection and extraction regimes will be applied directly to the warm well. Regimes will be

differentiated by utilizing different parameters based on injection and extraction rates and the duration of injection and extraction periods. The cold well will have a zero flowrate and not be in operation during this study. The hypothesis of the study is that initially when cold-water injection starts, the thermal energy stored proximal to the warm well will be pushed radially away from the borehole but not to a distance where it may not be recovered given all tested injection/extraction flowrates. Thermal energy that is initially farthest from the borehole will likely remain outside the capture zone during extraction, but temperature profiles will remain within 5°C above equilibrium conditions over the entire extent of the aquifer. Thermal recoveries during extraction will show a decreasing temperature trend over the push-pull testing simulation for all 1, 5, 10, 20, and 30-years periods.

3. THEORETICAL BACKGROUND AND NUMERICAL IMPLEMENTATION

Computer-based software is routinely used in groundwater transport problems and often used in shallow geothermal systems evaluations. This study will first utilize a finite difference method (FDM) software developed by the United States Geological Survey (USGS) as MODFLOW 2005, that is integrated into Visual MODFLOW Flex, which is a licensed software package developed by Waterloo Hydrogeologic for simulating solute and heat transport phenomena in porous media more effectively. There are several codes within this software package that aim to solve the partial differential equations related to fluid flow and heat transport. The comprehensive numerical code that will be used in this study is MT3DMS (Modular 3-Dimensional Transport Multi-Species), developed by Zheng and Wang (1999). MT3DMS is integrated into the software package and is used as a post-processor to simulate solute transport based on calculated flow fields from the numerical code MODFLOW 2005. When comparing the governing equations of solute and heat transport they are in fact mathematically similar and therefore the numerical code MT3DMS originally developed to simulate contaminant transport problems can also be used for heat transport modelling, described in more detail below. For this purpose, the corresponding parameters included in the partial differential equations of solute and heat transport (i.e., mechanical dispersion and molecular diffusion), need to be identified and defined accordingly to their respected thermal coefficients before the model is simulated.

3.1 Theoretical Background

The governing partial differential equation for transient groundwater flow and solute transport of Zheng and Wang (1999) and solved numerically with MT3DMS is given as,

$$\frac{\partial(\phi C^k)}{\partial t} = \frac{\partial}{\partial x_i}\left(\phi D_{ij}\frac{\partial C^k}{\partial x_j}\right) - \frac{\partial}{\partial x_i}(\phi v_i C^k) + q_s C_s^k + \sum R_n \quad (1)$$

where,

ϕ = porosity of porous medium, [dimensionless]

C^k = dissolved concentration of solute species (k), $[\frac{M}{L^3}]$

t = time, [T]

x_i = lateral distance in Cartesian coordinates, [L]

D_{ij} = hydrodynamic dispersion coefficient (includes molecular diffusion and mechanical dispersion); $D_{ij} = D_m + \alpha_s v_i$, $[\frac{L^2}{T}]$

D_m = molecular diffusion coefficient, $[\frac{L^2}{T}]$

α_s = dispersivity coefficient of solute, [L]

v_i = seepage velocity; in relation to Darcy flux (q_i) as, $v_i = \frac{q_i}{\phi}$, $[\frac{L}{T}]$

q_s = volumetric flowrate per unit volume of aquifer; fluid source or sink, $[\frac{L^3}{(T*L^3)}]$

C_s^k = concentration of species (k) from source or sink flux, $[\frac{M}{L^3}]$

$\sum R_n$ = chemical reaction term; $[\frac{M}{L^3 T}]$

The chemical reaction term is further broken down to Equation 3 of Zheng and Wang (1999) describing aqueous-solid phase sorption and first-order rate reaction as,

$$\sum R_n = -\rho_b \frac{\partial \bar{C}^k}{\partial t} - \lambda_1 \phi C^k - \lambda_2 \rho_b \bar{C}^k \quad (2)$$

where,

ρ_b= bulk density of porous medium, $[\frac{M}{L^3}]$

$\bar{C}^k$= concentration of species (k) sorbed on solids, $[\frac{M}{L^3}]$

λ_1 = first-order reaction rate of dissolved phase, $[T^{-1}]$

λ_2 = first-order reaction rate of sorbed phase, $[T^{-1}]$

The expansion of the left-side term in Equation 1 is given as,

$$\frac{\partial(\phi C^k)}{\partial t} = \phi \frac{\partial C^k}{\partial t} + C^k \frac{\partial \phi}{\partial t} = \phi \frac{\partial C^k}{\partial t} + q_s' C^k \quad (3)$$

where,

q_s'= $\frac{\partial \phi}{\partial t}$; rate of change in groundwater storage, $[T^{-1}]$

Substituting Equations 2 and 3 into Equation 1 and simplifying yields,

$$\phi \frac{\partial C^k}{\partial t} + \rho_b \frac{\partial \bar{C}^k}{\partial t} = \frac{\partial}{\partial x_i}\left(\phi D_{ij} \frac{\partial C^k}{\partial x_j}\right) - \frac{\partial}{\partial x_i}(\phi v_i C^k) + q_s C_s^k - \lambda_1 \phi C^k - \lambda_2 \rho_b \bar{C}^k \quad (4)$$

Reducing the left-side term in Equation 4 in the form of the retardation factor (R) yields,

$$R\phi \frac{\partial C^k}{\partial t} = \frac{\partial}{\partial x_i}\left(\phi D_{ij} \frac{\partial C^k}{\partial x_j}\right) - \frac{\partial}{\partial x_i}(\phi v_i C^k) + q_s C_s^k - \lambda_1 \phi C^k - \lambda_2 \rho_b \bar{C}^k \quad (5)$$

where,

$R = 1 + \frac{\rho_b}{\phi}\frac{\partial \bar{C}^k}{\partial C^k}$, [dimensionless]

$\frac{\partial \bar{C}^k}{\partial C^k}$ is representative of the distribution coefficient (K_d), $[\frac{L^3}{M}]$

Re-writing Equation 5 in simplified terms gives the solute transport equation as,

$$\left[1 + \frac{\rho_b K_d}{\phi}\right]\frac{\partial C^k}{\partial t} = div\left((D_m + \alpha_s v_i) grad C^k\right) - div(v_i C^k) + q_s C_s^k \quad (6)$$

Comparatively, Equation 6 is similar to the heat transport equation which includes mass conservation and the modes of heat transfer such as convection and conduction through the porous medium given by de Marsily (1986) as,

$$\left(\frac{\rho_m C_m}{\phi \rho_w C_w}\right)\frac{\partial T}{\partial t} = div\left(\left(\frac{\lambda_m}{\phi \rho_w C_w} + \alpha_h v_i\right) gradT\right) - div(v_i T) + \frac{q_h}{\phi \rho_w C_w} \quad (7)$$

where,

ρ_m = density of the porous medium, $[\frac{M}{L^3}]$

C_m = specific heat of the porous medium, $[\frac{J}{M*K}]$

ρ_w = density of water, $[\frac{M}{L^3}]$

C_w = specific heat of water, $[\frac{J}{M*K}]$

λ_m = thermal conductivity of porous medium, $[\frac{W}{L*K}]$

q_h = thermal flux injection/extraction, $[\frac{W}{L^3}]$

T = temperature of porous medium, $[K]$

There are several terms between Equations 6 and 7 that are mathematically equivalent when comparing solute and heat transport in porous media flow. Coefficient reformulations of these transport equations will serve as the input parameters for the MT3DMS solver. The following terms are compared and correlated below,

The retardation factor for solute sorption is equivalent to the thermal equilibrium term in Equation 7,

$$\left[1 + \frac{\rho_b K_d}{\phi}\right] \cong \left(\frac{\rho_m C_m}{\phi \rho_w C_w}\right) \qquad \text{where,} \quad K_d = \frac{C_m}{\rho_w C_w}\left[\frac{L^3}{M}\right] \quad (8)$$

Next, the molecular diffusion coefficient for solute transport is given as D_m and equivalent to the thermal diffusion term,

$$D_m = \frac{\lambda_m}{\phi \rho_w C_w}, \left[\frac{L^2}{T}\right] \quad (9)$$

The hydrodynamic dispersion term also includes the convective term given in both equations and their equivalence as,

$\alpha_s v_i = \alpha_h v_i$

$\alpha_s = \alpha_h$, $[m]$ (10)

Since the seepage velocity (v_i) remains the same, the solute and thermal dispersivities are equivalent.

The last term given in both equations represents the source/sink of energy or mass within the system. The source/sink term given by the solute transport equation represents the mass of solute being injected or extracted from the system. In the heat equation the term is given by the heat (energy) that is added or removed from the system. Their equivalence is shown as,

$q_s C_s^k = \frac{q_h}{\phi \rho_w C_w}$, $[\frac{M}{(T*L^3)}]$ (11)

COMSOL Multiphysics will also be used for this study for the same purposes as MODFLOW and MT3DMS. COMSOL utilizes the finite element method (FEM) to solve the same partial differential equations for coupled Darcy flow and heat transfer in porous material. The advantage that FEM has over FDM is that even though each software requires the discretization of cells to solve the transport equations, FEM is more computationally accurate due to its ability to form approximations of the transport equation at every point (node) of the domain rather than utilizing the difference between cells to determine the equivalent approximation at a specific discretized point. For this reason, FEM is able to handle sharper contrasts in dispersion and diffusion phenomena without being computationally inefficient.

3.2 Numerical Implementation

The 3D coupled thermo-hydrogeological numerical model is built and simulated in Visual MODFLOW Flex utilizing MODFLOW 2005 for groundwater flow and the solute transport code MT3DMS for equivalent heat transfer through convection and conduction as well as in COMSOL Multiphysics utilizing Darcy physics and heat transfer through porous material interfaces. The two software packages will be compared against each other for validation purposes. The developed model is composed of three layers defining a confined aquifer with fine sand as the aquifer medium and semi-impermeable clay layers for the confining units. The thickness of the aquifer is 50 m, and each confining layer is 30 m in thickness. Detailed hydraulic and thermophysical properties of the fluid and rock formations are given in Table 2.1.

A doublet well open-loop system featuring one cold-well for injection and extraction as well as one warm-well for injection and extraction is configured. In both models, the domain of the model uses a grid size of [200 m, 250 m, 110 m] and the cold-well is located at coordinates (85 m, 100 m) and the warm-well is located at (165 m, 100 m) from the left (West) boundary, as shown in Figures 3.1 and 3.2. Additionally, Figures 3.3 and 3.4 show a closer extent of the discretized cells near the warm well highlighted by the red rectangle in Figures 3.1 and 3.2. The wells extend from the ground surface down to the base of the aquifer. The screen length covers the total aquifer thickness. For the COMSOL software, both cold and warm-wells are given as a line source and use a mass flow rate of injection and extraction equivalent to MODFLOW's volumetric flow rate.

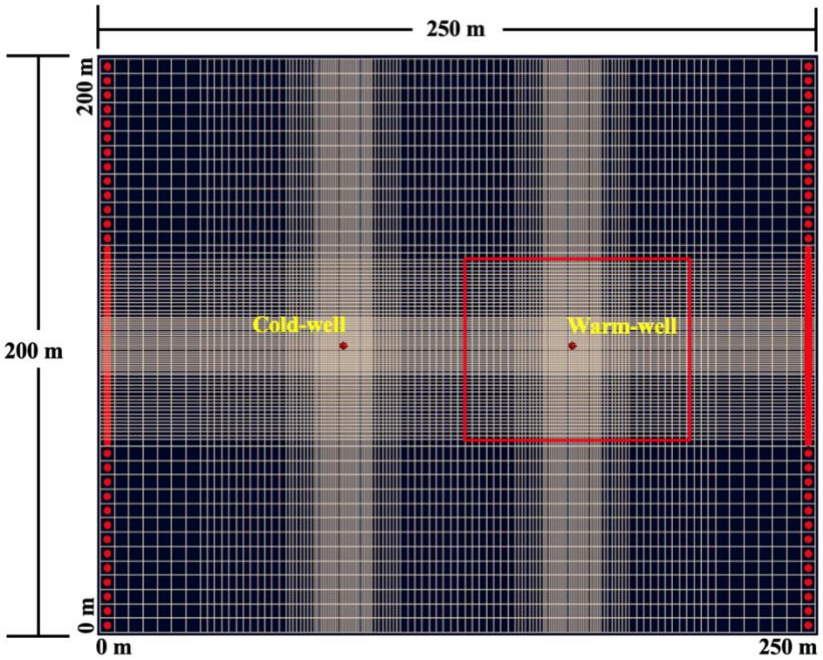

Figure 3.1 Grid domain built in MODFLOW illustrating grid and well spacing. The outermost grid cells along boundaries are [5 m, 5 m] and cells proximal to the wells are [0.63 m, 0.63 m]. The red dots on the left and right boundaries represent constant hydraulic heads of 100 m.

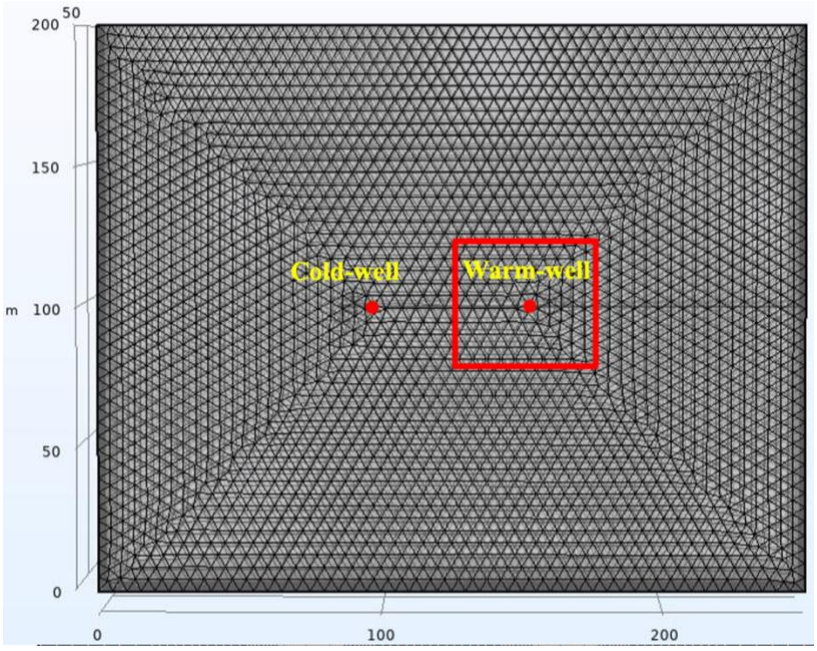

Figure 3.2 Grid domain built in COMSOL illustrating grid and well spacing. The outermost grid elements (triangles) along boundaries are 5 m and elements proximal to the wells are 0.2 m.

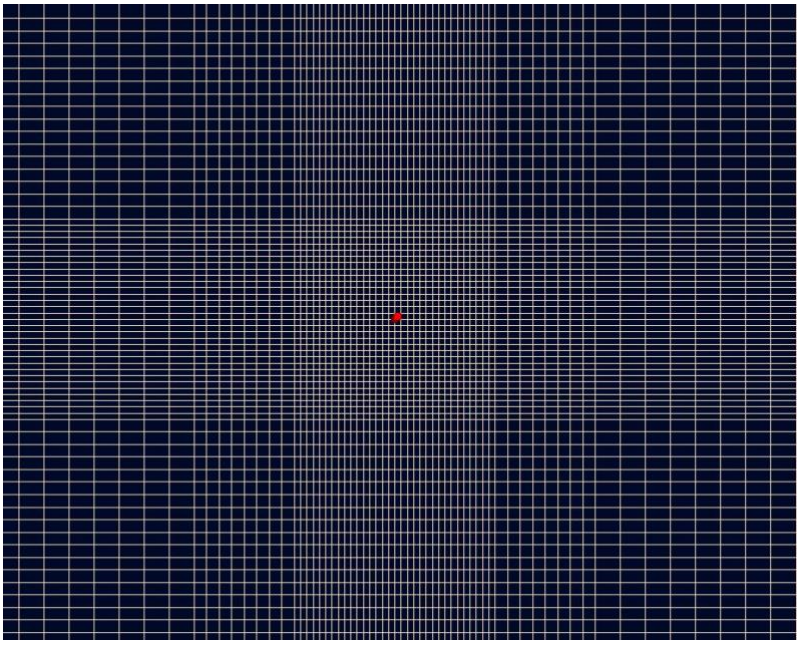

Figure 3.3 MODFLOW grid domain surrounding the warm-well (equivalent grid spacing applied the cold-well). The outermost grid cells are [2.50 m, 2.50 m] and cells proximal to the wells are [0.63 m, 0.63 m].

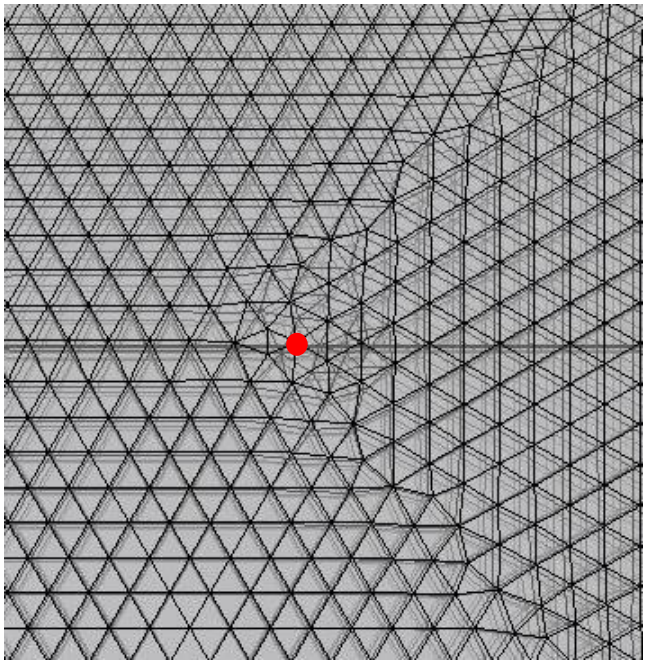

Figure 3.4 COMSOL Grid domain surrounding the warm-well (equivalent grid spacing applied the cold- well). The outermost grid elements along boundaries are 2 m and elements proximal to the wells are 0.2 m.

The following assumptions and conditions are applied to the MODFLOW and COMSOL models:

1. No groundwater flow across the domain. The hydraulic heads at the West (x = 0 m) and East (x = 250 m) boundaries are 100 m.
2. All modes of heat transfer are considered in the numerical simulations. This includes convection in porous media and lateral and vertical heat conduction. For MODFLOW, solute diffusion resembles conductive heat within the porous medium and into the confining layers.
3. The initial temperature of the aquifer and upper and lower confining layers is 285.15 K (12 °C).
4. Due to low temperature fluctuations of the system (less than ~20 °C difference between lowest and highest values), temperature effect on dependent parameters such as viscosity, density, and heat capacity of the medium and water are assumed to be minimal and remain constant.

4. METHODOLOGY

4.1 ATES Calibration Model and 5-Yr Operation Test

Creating and calibrating a theoretical numerical model for a two-well doublet ATES system with a simulated operation time of five years will be the foundation of the study. Table 4.1 provides the five-year operational schedule for well injection and extraction scenarios. The proceeding case studies will utilize this pre-existing model and its aquifer conditions at t = 5 years (1825 days) as the initial conditions. The purpose here is to set a benchmark and evaluate several operational scenarios to understand their effect on transient temperature distributions in porous media after the system's five years in operation.

The initial simulation of this task will provide a reference point regarding the operational efficiency and accuracy of the system. Adjusting the model domain in conjunction with using different advection solvers in the numerical code will play a role in the model's output accuracy. Initial boundary conditions as well as input parameters regarding thermos-hydrogeologic fluid and physical properties will follow similar studies carried out by Ganguly and Kumar (2017), Hecht-Mendez (2010), Kim (2010), and Lee (2008). Adjustments to the model domain include the grid mesh set-up, configuring two different grid domain sizes and their respected cell/element grid spacings (fine grid spacing proximal to the wells and a coarser spacing further from the wells). For MODLFOW, two different advection solvers will be used to run the simulation namely, central finite difference method (CFD) and total variation diminishing (TVD). The contributing differences between CFD and TVD solvers is their ability to solve numerical dispersion while maintaining minimal mass balance errors and reduced artificial oscillations. Under advection dominated problems where dispersion is more of a concern compared to

diffusion/conduction, CFD has generally led to develop less accurate results due to its susceptibility in increasing artificial oscillations caused by using previous calculated values based on cell nodal points. This is largely a concern when dealing with a sharp contrast in the thermal or solute front where there is little gradual gradient in the transport zone. Comparatively, TVD solves the advection term independently from all other terms in the transport equation since it follows particle-based methods, therefore reducing the likelihood of repeating oscillations in advection problems (Waterloo Hydrogeologic).

5-Year ATES Operation Schedule

	Injection/Extraction Rate (m^3/day)					**Injection Temperature (K)**				
Month	1-2	3-5	6-8	9-11	12	1-2	3-5	6-8	9-11	12
Cold Well	100	0	-100	0	100	278.15	-	-	-	278.15
Warm Well	-100	0	100	0	-100	-	-	298.15	-	-

Table 4.1. Cold-water injection during months 12-2 and warm water injection during months 6-8, repeating for a total of 5 years of operation. Minus sign (-) in front of rate indicates extraction.

The expectation is that the numerical model for the five-year operation of the simulated ATES system will provide the transient temperature distributions in the confined aquifer between the warm and cold injection and extraction wells. It will take more than one simulated year but less than five for the aquifer to effectively store warm water as thermal energy and for the groundwater temperature surrounding the warm well to increase for optimal use. Temperatures near the warm well will not exceed more than 30 °C (303.15 K). Temperatures near the cold-well will remain above 5 °C (278.15 K).

4.2 ATES 5-Yr Operation Test and Transition to 30-Yr “Idle” Period

Establishing a base case scenario using an idle period simulation will offer a benchmark for comparison when simulating the effect of cold-water injection on transient temperature

distributions in the final study. This study aims to assess how heat in the aquifer dissipates and is transferred through the aquifer and confining layers over time, with no well injection and extraction.

The initial conditions for the idle period simulation include the transient temperature distributions and groundwater flow regime developed during the first procedure when calibrating the model to simulate an ATES system in five-years of operation. When the system is in idle, there is no thermal injection or extraction from the system during the entire simulation over a 30-year period. Refer to Table 4.2 for the "Idle" period operational schedule. The simulation will begin at zero days and will run under natural conditions to demonstrate all modes of heat transfer through porous media. Temperature distribution data will be taken over 12 stress periods of one month each over the 30-year time interval. Each stress period is subdivided into time steps of 1 day (365 total time steps). Over the thirty-year simulation there will be a total of 360 stress periods of one month each with 10,950 total time steps. Temperatures of the porous media as well as the upper and lower confining clay layers will be recorded for the 1, 5, 10, 20, and 30-year time markers. The results of the idle study will provide the benchmark dataset that will be used to compare with the temperature distributions developed from the next study using the remedial cold-water push-pull approach. The same model domain and advection solvers used in the first study will remain the same for this study.

5-Year ATES Operation Schedule and Transition to 30-Year Well Shut-down Idle Period

		Warm Well		Cold Well	
	Time	Injection/Extraction Rate (m^3/day)	Injection Temperature (K)	Injection/Extraction Rate (m^3/day)	Injection Temperature (K)
ATES 1-Yr (Repeat schedule for 5 years)	1-2 (mo.)	-100	-	100	278.15
	3-5 (mo.)	0	-	0	-
	6-8 (mo.)	100	298.15	-100	-
	9-11 (mo.)	0	-	0	-
	12 (mo.)	-100	-	100	278.15
30-Yr "Idle" period	1 (yr.)	0	-	0	-
	5 (yrs.)	0	-	0	-
	10 (yrs.)	0	-	0	-
	20 (yrs.)	0	-	0	-
	30 (yrs.)	0	-	0	-

Table 4.2. Time is given in months (mo) for the ATES 1-Yr cycle which repeats for five total years before both warm and cold wells are shut off and the idle period starts.

The expectation of the idle period simulation is that the stored thermal energy surrounding the warm-water injection well will form radially outward away from the well with decreasing temperatures at distance from the center of the borehole. Since there is no pumping during this time, thermal energy will slowly dissipate through the porous media due to the ambient groundwater minimal flow patterns with a small; almost negligible amount of heat conducting into the confining clay layers. Groundwater temperatures will resemble the natural aquifer temperatures (before ATES deployment) at a distance where the thermal front does not propagate further from the warm-well in time. Cooler temperature distributions will remain steady near the cold-well and will also form radially outward from the cold well with minimal changes in temperature away from the well. There will be a temperature gradient between the warm and cold wells where the temperature distribution halfway between the two wells will be slightly warmer than that of the ambient groundwater flow. The temperatures of both confining

layers will gradually decrease as the thermal energy stored in the clay layers will leak back into the aquifer over the 30-year period.

4.3 Cold-water Injection during Push-Pull Remedial Approach

This study focuses on capturing the feasibility of cold-water injection and groundwater extraction during a series of push-pull operations to simulate potential remedial strategies for an aquifer having existing stored thermal energy. Simulations during this study aim to evaluate the most effective scenario (based on pumping rate and injection temperature), that will minimize thermal energy stored in the aquifer over time, seeking to bring the aquifer back to pre-existing ATES conditions (ambient groundwater temperatures).

This push-pull study will be used to evaluate the effects of cold-water injection on the temperature of the system through time. Its purpose is to measure scenarios that can most effectively reduce the thermal energy in the aquifer to bring it back to steady state conditions before the ATES system was implemented in the study area. This study will include 24 cases that are each differentiated by various injection and extraction rates paired with different cold-water injection temperatures only in the warm-well itself. Cold-water injection does not include the use of the cold-well. Cold-water injection temperatures will not exceed the temperature of the aquifer under natural conditions (less than 15°C). The following stress periods and time steps for recording transient temperature distributions of the aquifer system and thermal recoveries at the warm-well are below:

1. One year of operation: 12 stress periods of one month each. Each stress period is subdivided into time steps of 1 day (365 total time steps).
2. Five years of operation (5-yr ATES cycle): 60 stress periods of one month each. Each stress period is subdivided into time steps of 1 day (1,825 total time steps).

3. Ten years of operation (5-yrs ATES, 5-yrs cold-injection): 120 stress periods of one month each. Each stress period is subdivided into time steps of 1 day (3,650 total time steps).
4. Twenty years of operation (5-yrs ATES, 15-yrs cold-injection): 240 stress periods of one month each. Each stress period is subdivided into time steps of 1 day (7,300 total time steps).
5. Thirty years of operation (5-yrs ATES, 25-yrs cold-injection): 360 stress periods of one month each. Each stress period is subdivided into time steps of 1 day (10,950 total time steps).

The operational schedule for the push-pull simulation is provided in Table 4.3. The injection and extraction rates vary from 50 m^3/day in cases 1 through 4, 100 m^3/day in cases 5 through 8, 150 m^3/day in cases 9 through 12, 200 m^3/day in cases 13 through 16, 250 m^3/day in cases 17 through 20, and 300 m^3/day in cases 21 through 24. Temperature ranges between 5 to 10 °C will be applied to all extraction rates to understand how coupled cold-water injection temperatures and pumping rate influence the equilibrium of the aquifer.

Table 4.3 Cold-Water Push-Pull Operation Schedule for Warm Well ATES Injection/Extraction

	Injection/Extraction Rate (m^3/day)				**Injection Temperature (°C)**			
Month	1-3	4-6	7-9	10-12	1-3	4-6	7-9	10-12
Case 1	50	-50	-50	50	5	-	-	5
Case 2	50	50	-50	50	5	5	-	5
Case 3	50	50	-50	50	5	10	-	5
Case 4	50	-50	-50	50	10	-	-	10
Case 5	100	-100	-100	100	5	-	-	5
Case 6	100	100	-100	100	5	5	-	5
Case 7	100	100	-100	100	5	10	-	5
Case 8	100	-100	-100	100	10	-	-	10
Case 9	150	-150	-150	150	5	-	-	5

Table 4.3 Continued. Cold-Water Push-Pull Operation Schedule for Warm Well ATES Injection/Extraction.

Case 10	150	150	-150	150	5	5	-	5
Case 11	150	150	-150	150	5	10	-	5
Case 12	150	-150	-150	150	10	-	-	10
Case 13	200	-200	-200	200	5	-	-	5
Case 14	200	200	-200	200	5	5	-	5
Case 15	200	200	-200	200	5	10	-	5
Case 16	200	-200	-200	200	10	-	-	10
Case 17	250	-250	-250	250	5	-	-	5
Case 18	250	250	-250	250	5	5	-	5
Case 19	250	250	-250	250	5	10	-	5
Case 20	250	-250	-250	250	10	-	-	10
Case 21	300	-300	-300	300	5	-	-	5
Case 22	300	300	-300	300	5	5	-	5
Case 23	300	300	-300	300	5	10	-	5
Case 24	300	-300	-300	300	10	-	-	10

The expectation of the push-pull simulation is that at the start of cold-water injection the thermal energy stored near the warm-water well will be pushed further from the borehole but will remain in the capture zone to be recovered. Lower injection and extraction rates may limit the movement of the thermal front dispersed through the porous media but will increase the time it takes for the aquifer to return to pre-ATES system conditions. The opposite is to be expected for higher injection and extraction rates, though there is the potential for the thermal front to move far enough away from the warm-well to a point outside the capture zone where the thermal energy cannot be captured most effectively, leaving residual heat to disperse in the aquifer over time. Thermal energy that is above 15°C that is initially farthest from the borehole will likely remain outside the capture zone during extraction, but temperature profiles across the aquifer's extent will remain within 5°C above equilibrium conditions.

5. RESULTS AND DISCUSSION

5.1 Testing of MODFLOW's Numerical Advection Solver

The numerical model was tested and calibrated against the two advection solvers, CFD and TVD, to ensure the most effective accuracy in generated results for each these studies. The initial phase included calibrating the model for a two-well doublet ATES system with a simulated operation time of five years to serve as the benchmark for future studies. The solvers were further compared in the ATES 30-Yr idle period and cold-water injection scenarios. Figure 5.1 provides a visualization of the discrepancy between the two advection solvers given in MODFLOW and MT3DMS for the ATES 5-Yr operation study.

Based on Figure 5.1, one observation can be made about the temperature distribution near the cold wellbore. CFD temperatures appear to converge to a value close to 278 K (4.85°C), regardless of simulated time. Conversely, TVD handles solving near the wellbore more effectively since there should be a temperature differential developed through time due to the cold-water injection and extraction, similarly to the warm-well side at 165 m. This difference is most likely due to the sharp gradient near the cold-well which CFD may have difficulty calculating dispersion in this region. Figure 5.2 illustrates the comparison between the solvers based on the 30-Yr idle period case, which shows slightly more variability between TVD and CFD at both the cold and warm-wells. Lastly, Figure 5.3 shows their comparison during cold-water injection and extraction, where there are most noticeable discrepancies proximal to the warm-well. For this reason, the TVD method will be used in the MODFLOW and MT3DMS simulations for all studies.

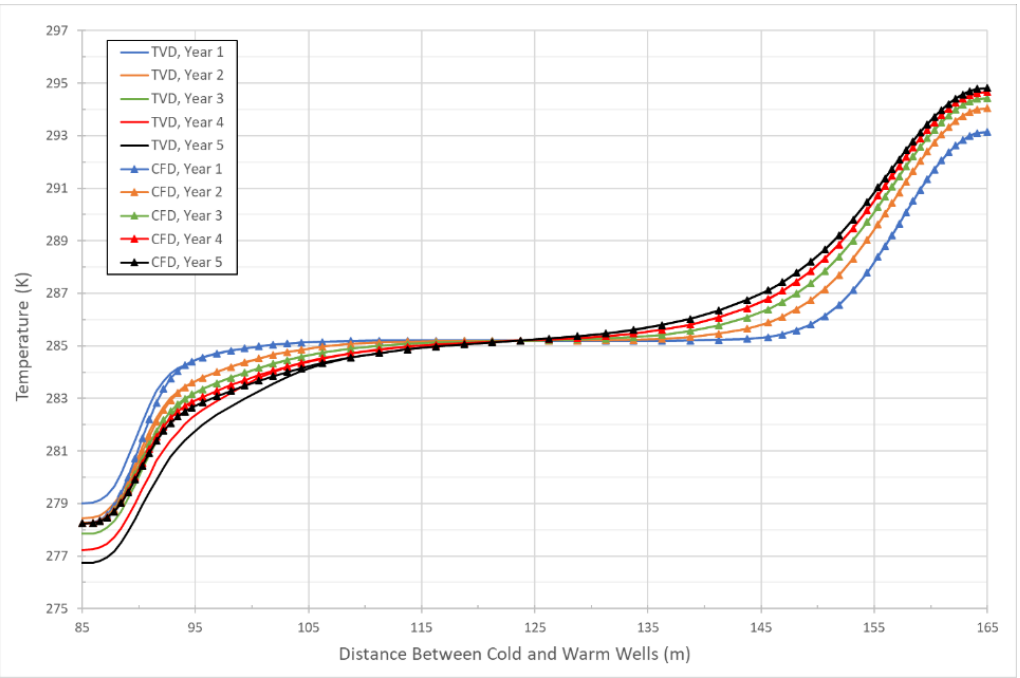

Figure 5.1 ATES 5-Yr operation study comparing TVD and CFD solutions of temperature distribution between doublet wells in the aquifer (layer 2).

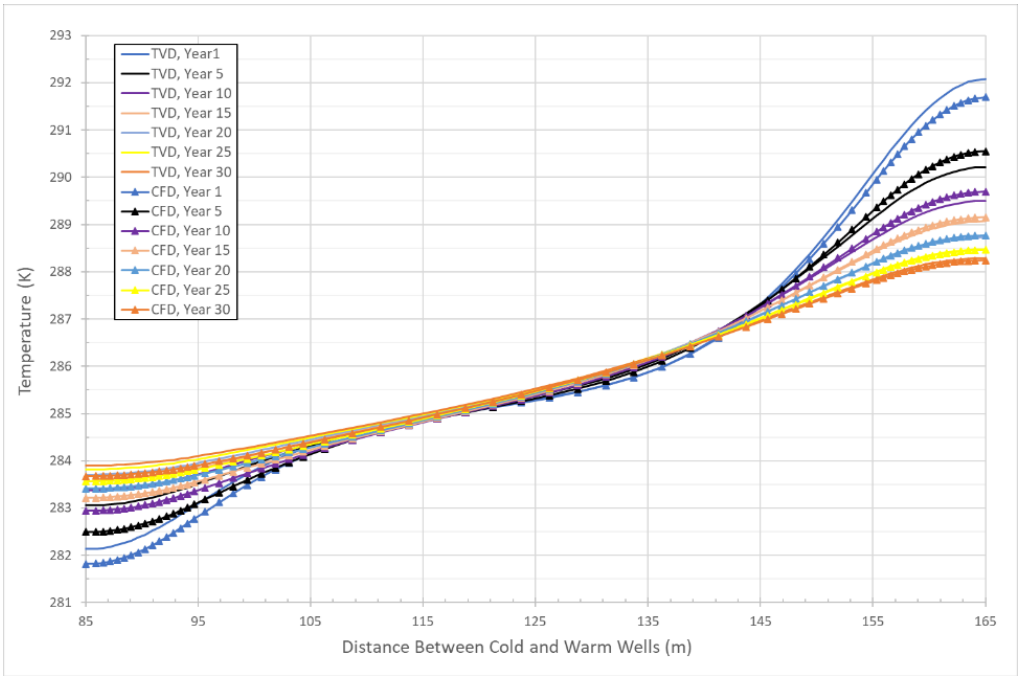

Figure 5.1.1 ATES 30-Yr idle operation study comparing TVD and CFD solutions of temperature distribution between doublet wells in the aquifer (layer 2).

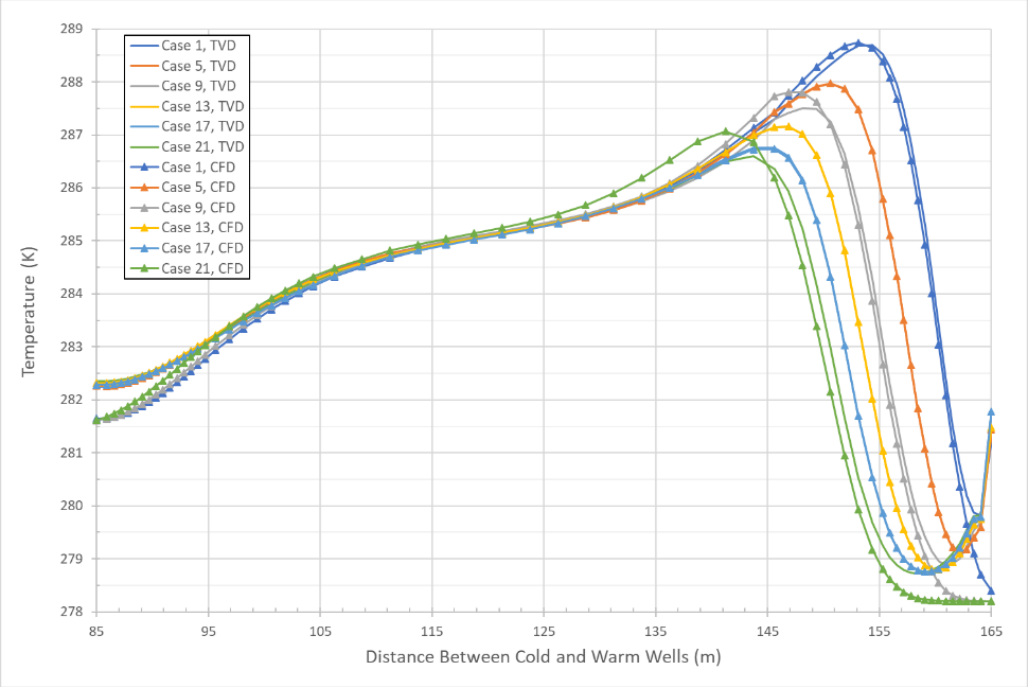

Figure 5.1.2 ATES cold-water injection operation study comparing TVD and CFD solutions of temperature distribution between doublet wells in the aquifer after 1 year with an injection/extraction rate of 50 m^3/d (layer 2).

5.2 ATES 5-Yr Operation Test

The ATES 5-Yr study served as the basis to the proceeding studies due to the priming of the aquifer, where enough thermal energy needed to be injected into the aquifer generating high enough temperature anomalies to study thermal dispersion over time, and to perform the remedial work in push-pull testing. The study did require more than one simulated year of injection and after five years there was large enough differences in temperatures between the cold and warm wells to effectively observe thermal dispersion and enough energy stored in the aquifer for optimal use. Figures 5.2 (a) to 5.2 (d) in Appendix B show the comparison between MODFLOW and COMSOL temperature distributions with distance between wells and distance away from the warm-well with time for both layer 1 (upper confining clay) and layer 2 (aquifer), respectively. In all cases, the maximum temperature did not exceed more than 30°C (303.15 K),

though temperatures near the cold-well reduced below 5°C (278.15 K) to 275.1 K (1.95°C) which was lower than hypothesized.

Figures 5.2 (a) and (b) show a relatively fine correlation between MODFLOW and COMSOL results of the temperature distributions between the wells in layers 1 and 2. In layer 2, the largest temperature differences occur near the wellbores with a maximum difference of 1.58°C occurring in the first year at the warm-well and a maximum difference of 1.64°C after five years at the cold-well. In this layer, the average maximum temperature after five years is 22.2°C at the warm well and average lowest temperature is 2.78°C at the cold-well. It was expected that the lowest temperature in the aquifer would not reduce lower than 5°C, though it is appropriate to find that this is not the case given that the cold storage develops over time and contributes to a decreasing temperature distribution near the wellbore. In layer 1, the largest temperature differences are smaller, where there is a 0.03°C difference at both the warm and cold-wells after five years, indicating no significant concerns between modeling approaches. In this layer, the average maximum temperature is 12.55°C at the warm-well and average lowest temperature at the cold-well is 11.74°C after five years, indicating that there is subtle influence of conduction into the confining layer due to thermal injection in the aquifer, where the temperatures remain <1°C from ambient conditions.

Figures 5.2.1 (e) and (f) show the temperature distributions with respect to time at various distance probes between wells and away from the warm well for each layer. Between wells in layer 2, the first observation is that there is no thermal interference at the midpoint (x = 40 m), indicating that the thermal front due to both cold and warm injection does not influence either region. At x = 40 m, the initial temperature is ambient (12°C) and after five years it remains about the same reaching 12.055°C, a 0.055°C difference. However, at x = 70 m, the

temperature increases to 17.25°C after 5 years, a 5.25°C difference from ambient, indicating that the thermal front migrates away from warm well, with significant influence (>5°C), though this reduced gradually which can be seen at x = 60 m. Similarly, this phenomenon also occurs between wells in layer 1, where there is only a 0.007°C above ambient increase at x = 40 m and 0.32°C increase at x = 70 m after five years, and reducing significantly at x = 60 m.

Figures 5.2 (c) and (d) show roughly the same correlation between MODFLOW and COMSOL temperature distribution results away from the warm-well in layers 1 and 2. In both layers, given symmetry and the proximity to the wellbore there is negligible temperature variations in the average maximum temperature after five years from that given in Figures 5.2 (a) and (b). Based on (c) and (d), two observations can be made. First, in both layers, the thermal front due to storage at the warm-well does not migrate too far from the source after five years. When observing the temperatures away from the warm well in Figures 5.2.1 (g) and (h), the thermal front significantly drops off after about 15-20 m and approaches equilibrium conditions in both layers well before 5 years. In layer 2, at x = 20 m, the temperature increases to 13.55°C, a 0.55°C difference and at x = 40 m, the temperature slightly increases to 12.1°C, a 0.1°C difference above ambient. In layer 1, at x = 20 m, the temperature increases to 12.11°C, a 0.11°C difference and at x = 40 m, the temperature slightly increases to 12.01°C, a 0.01°C difference above ambient. The thermal plume remains very proximal to the warm-well during the full ATES operation and there is no significant heat loss to the confining layers.

5.3 ATES 30-Yr “Idle” Period

The idle period establishes how the residual heat will disperse throughout the aquifer and into the confining layers over 30 years. The approach towards equilibrium is assessed with main concerns regarding how heat is lost to the surrounding regions away from the warm-well and

into the confining layers and provides insight into the duration of this dispersion process. The shut-down of both wells during this study is followed by how the aquifers natural properties control the release of transient temperature distributions away from the wellbores, more importantly the warm-well. Similarly, to the first study, Figures 5.3 (a) to 5.3 (d) in Appendix C show the comparison between MODFLOW and COMSOL temperature distributions with distance between wells and distance away from the warm-well with time for both layer 1 and layer 2, respectively.

Based on Figures 5.3 (a) and (b), there is strong evidence showing that the thermal energy stored near the warm-well begins to decrease at a faster rate within the first 10 years after the shutdown, but then gradually slows as temperatures between wells and away from the warm-well approach within 2°C to 3°C above ambient. In layer 2, after one year of shutdown the average temperature at the warm-well decreases to 19.42°C, down 2.78°C from the peak temperature of 22.2°C from the fifth year of ATES operation, previously. The average temperature at the cold-well increases to 9.33°C, up 6.55°C from the lowest temperature of 2.78°C from the fifth year of ATES operation, a significant increase. After idling for five years, the temperature at the warm-well decreases to 17.67°C, another 1.75°C reduction. And the temperature at the cold-well increases to 10.16°C, another 0.83°C increase. After 30 years, the average temperature at the warm-well reaches 14.15°C, still 2.15°C above ambient though within the 5°C threshold for concern. At the cold-well the average temperature warms to 11.41°C, 0.59°C below ambient. In layer 1, after the first year of shutdown, the average temperature at the warm-well increases to 12.71°C, up 0.16°C from the five-year temperature of ATES operation. The temperature at the cold-well increases to 11.85°C, up 0.11°C from the five-year lowest ATES temperature. After continued idle for five years, the temperature at the warm-well

increased to 12.75°C, just another 0.04°C. The temperature at the cold-well started to decrease to 11.83°C, down only 0.02°C. After 30 years, the temperature at the warm-well reached 12.95°C, 0.95°C above ambient. At the cold-well, the temperature continued to reduce to 11.76°C, 0.24°C below ambient.

This brings up two interesting observations. Firstly, the increase in temperature in the confining layer at both the warm and cold-wells was not expected, rather the opposite was hypothesized. Instead of the heat dissipating out from the confining layer and into the aquifer, the thermal energy stored in the aquifer continued to conduct through the confining layer, continuously in the region above the warm-well and initially in the region above the cold-well. However, the second observation indicates that after the fifth year of this idle period the heat did begin to dissipate out of the confining layer above the cold-well, but the rate that this occurred was not significant. This is most likely due to the low thermal gradient surround the cold-well region.

Similarly to the ATES 5-yr study, Figures 5.3.1 (e) and (f) show the temperature distributions with respect to time at various distances between wells and away from the warm-well for layers 1 and 2. In layer 2, after 30 years the temperature between wells at x = 40 m is 12.4°C, 0.4°C above ambient. This shows slight indication that the warm front influences the region as the temperature slightly increases over time due to the thermal energy dispersed from the warm-well. At x = 70 m, the temperature after one year is 16.72°C, down 0.53°C from 17.25°C due to the ATES 5-year system. The average temperature then decreases to 13.84°C after 30 years, down 3.41°C from that of the ATES operation at 5 years, but still 1.84°C above ambient. Conversely, in layer 1, the temperature at x = 40 m increases slightly to 12.17°C after 30 years, only 0.05°C above the ATES 5-year. At x = 70 m, the temperature continues to rise to

12.85°C, 0.52°C above the ATES 5-year. This indicates that the confining layer is warming due to the heat dispersed from the warm-well.

Based on Figures 5.3 (c) and (d), it appears that in layer 2 the thermal plume remains relatively stationary (within 20 m from the warm-well) with time however the heat is reduced significantly over 30 years, contributing to heat gained in the confining layers. In layer 1, the temperature proximal to the warm-well gradually increases with time, as shown previously. When observing the temperatures away from the warm well in Figures 5.3.1 (g) and (h), in layer 2, the thermal front significantly drops off at a distance of approximately 15 m from the warm-well, but the temperature remains elevated within this distance for all 30 years, with an average temperature of 13.31°C at t = 30 years, slightly down from the 13.55°C given by the ATES 5-year study. At x = 40 m, the temperature increases to 12.55°C, a 0.45°C difference above the ATES study. At x = 60 m and 80 m, there is little sign of the thermal front migrating into this region away from the warm-well. In layer 1, the temperature gradually increased to 12.55°C after 30 years, 0.44°C above the ATES study at 5-years. There is heat added to the confining layer even at x = 40 m, where the average temperature after 30 years is 12.14°C, 0.13°C higher than the ATES 5-year study.

There appears to be a rather significant conductive path for heat to influence the temperature of the confining layer, more than expected. Initially, heat was added to the confining layer above the cold-well, but with time this was reduced due to the cold-water front dispersing into the upper layer. The thermal front in the aquifer does not migrate more than 20 m from the warm well, however there is slight thermal influence between the wells 30 years after the shut-down.

5.4 Cold-Water Injection Push-Pull Testing

Evaluating the most effective pumping rate and injection temperature to minimize residual heat in the aquifer encompasses numerous push-pull test cases. Simulations aim to understand the effects of cold-water injection on the temperature of the system through time. After 24 cases were tested pertaining only to MODFLOW simulations (the COMSOL model was not used in this study given the low discrepancy between the two models), there became clear indication of what injection regime worked most efficiently to restore the aquifer back to equilibrium conditions; pre-ATES deployment. Effectiveness was gauged based on a few factors such as, the duration of time needed to reduce thermal energy stored in the warm-well region, the amount of injection and extraction needed which is dictated by volumetric flowrate, and the cyclic regime (duration of push-pull tests). The assessments were made based on the temperature distributions in layer 2 given by time intervals of push-pull testing after 1, 5, 10, 15, and 25 years. The focus is specifically in layer 2, given that the confining layers are not significantly influenced by thermal effects to be a major concern for this part of the study. Results are shown in Appendix D, Figures 5.4 (a) to (d) presenting temperature distributions with distance with respect to one year of testing, Figures 5.4.1 (a) to (d) for 5 years, Figures 5.4.2 (a) to (d) for 10 years, Figures 5.4.3 (a) to (d) for 15 years, and Figures 5.4.4 (a) to (d) for 25 years of testing.

After the first year of cold-injection, based on Figures 5.4 (a) to (d), an injection rate of 300 m^3/d with a temperature regime of (5,5,-,5) (Case 22) is a significant method for reducing residual heat in the aquifer between wells. The maximum temperature in the aquifer after injection is 13.25°C, 28.8 m away from the warm-well. The temperature at the midpoint is 12.55°C, 0.55°C above ambient. A similar method to reduce residual heat is case 23 maintaining a 300 m^3/d injection with a temperature regime of (5,10,-,5). The maximum temperature in the

aquifer after injection is 13.26°C, 28.8 m away from the warm well with a midpoint temperature of 12.6°C, 0.6°C above ambient. The least effective is case 4 where injection is 50 m^3/d with a temperature regime of (10,-,-,10) as the maximum temperature only reduces to 15.54°C, 10.6 m away from the warm-well. However, the temperature at the midpoint is 12.19°C, 0.19°C above ambient. During the one year of injection, reducing residual heat is best accomplished through injecting at a higher rate of 300 m^3/d at 5°C during the first six months and last three months of testing. The least effective method is due to the lowest injection rate which does not reduce or move the thermal plume nearly as much and contributes to longer remediation durations.

After 5 years of cold injection, evaluating Figures 5.4.1 (a) to (d), shows an injection rate of 250 m^3/d with a temperature regime of (5,-,-,5) (Case 17) is the most effective method for reducing residual heat in the aquifer. The maximum temperature between wells after injection is 11.88°C, 40 m away from the warm well. The temperature at the midpoint is also 11.88°C, 0.12°C below ambient. Case 21 shows a similar trend to case 17, however, given the little temperature difference between the two the amount of water use due to the higher flow rate does not constitute being more efficient. A moderate approach follows case 11 which has an injection rate of 150 m^3/d with a temperature regime of (5,10,-,5). The maximum temperature is 11.9°C, 49 m from the warm-well and the midpoint temperature is 11.4°C, 0.6°C below ambient. The least effective method is case 4 due to its low injection rate of 50 m^3/d and higher temperature injection regime of (10,-,-,10), where the temperature is reduced to 12.73°C at the maximum level and midpoint temperature is 12.34°C. After 5 years, the slightly higher flowrate of 250 m^3/d while having an injection temperature regime of 5°C in the first and last three months of each year serves to be most effective. The trend continues in the near term that shows having a lower flowrate does not influence the stored heat nearly as much. Additionally, one key

observation can be made about the injection temperature regime in that it has less of an impact on reducing thermal energy in the aquifer when compared to the injection flowrate. Push-pull is more effective in the transport of groundwater and associated convective heat to reduce temperature distributions compared to lowering them via injection temperature itself.

After 10 years of push-pull testing, Figures 5.4.2 (a) to (d), shows an injection rate of 100 m^3/d with a temperature regime of (5,-,-,5) (Case 5) to be most effective in reducing residual heat. The maximum temperature in the aquifer after injection is 11.74°C, 44 m away from the warm well. The temperature at the midpoint is also 11.65°C, 0.35°C below ambient. Conversely, having too high of a flowrate after 10 years of push-pull testing leads to too much cooling of the aquifer which can be attributed to a waste of energy. This observation is based on case 22 where a flowrate of 300 m^3/d with a temperature regime of (5,5,-,5) reduces the aquifer temperature to 6.3°C, 5.7°C below ambient. This reduction surpasses the 5°C threshold for concern for this study and is an example of over-injection.

There is a noticeable transition in flowrate effectiveness after 15 years of push-pull testing. Based on Figures 5.4.3 (a) to (d), it appears that lower flowrates become more efficient at this point in time due to over-cooling caused by higher flowrates which reduce much of the thermal energy in the aquifer before the 5 and 10-year timeframes. After 15 years, the most effective method is case 3 with a flowrate of 50 m^3/d and temperature regime of (5,10,-,5) as it reduces the maximum aquifer temperature to 11.79°C, 59 m away from the warm-well and the midpoint temperature is 11.25°C, 0.75°C below ambient. The least effective is case 22 due to the high injection rate of 300 m^3/d where the midpoint temperature significantly drops to 5.95°C, 6.05°C below ambient and even further below the acceptable threshold.

Lastly, after 25 years of cold-injection, based on Figures 5.4.4 (a) to (d), an injection rate of 50 m^3/d with a temperature regime of (5,-,-,5) (Case 1) is most effective. The maximum temperature in the aquifer after injection is 11.9°C, 57 m away from the warm-well. The temperature at the midpoint is 11.75°C, just 0.25°C below ambient. Case 4 is a significant method as well, showing very similar trends to case 1.

It appears that higher injection rates within the first 1 to 5 years of push-pull testing have the largest impact on reducing the residual heat left behind by the ATES system. After the first year, an injection rate of 300 m^3/d with a temperature regime of (5,5,-,5) is most effective, however the aquifer temperature remains 0.55°C above pre-ATES deployment conditions. After five years, a reduced flowrate of 250 m^3/d works best as the maximum temperature reduces to 0.12°C below ambient. Effective flowrates continue to decrease with time as 100 m^3/d is best after 10 years, and 50 m^3/d after 15 and 20 years. Higher injection rates in testing after 10 years leads to over-cooling of the aquifer, therefore wasting water resources and energy. The thermal energy stored proximal to the warm-well does not maintain the same region during push-pull testing as expected, as the thermal front is pushed to a distance of around 50 m from the warm-well after around 5 years. This influence is not of major concern since this uncaptured energy contributes to the warming of the cold-well region over time. Temperature regimes do not play a significant role in contributing to thermal remediations, this is due to convective processes overriding conductive transport.

6. CONCLUSIONS

In this study, it can be determined that MODFLOW and MT3DMS are useful in simulating coupled groundwater flow and heat transport through porous material given the correlation of coefficients between species in solute transport and thermal coefficients in heat transfer. The MODFLOW advection solver needed for most accurate deliverables within this study is TVD as it can approximate solutions near the wellbores more effectively due to the temperature gradient developed through time due to the cold-water injection and extraction, and similarly to the warm-well. The MODFLOW software was able to produce comparable results to the COMSOL software to a good degree with no significant discrepancies when simulating the ATES 5-year and 30-year idle period studies. This provided the appropriate usefulness to continue to use MODFLOW as a solving tool for the purpose of this study. Additionally, one concerning point to these models is the degree of influence that grid or mesh configurations have on the precision of the approximated solutions, more notably near the wellbore regions. Optimization studies focusing on highest discretization of the domain space without sacrificing significant computation time while ensuring effective results is necessary for future work.

The ATES 5-year study provided an optimal priming of the aquifer to then be utilized for the idle period and cold-water injection scenarios. Expectations of the ATES 5-year system were met as the maximum temperature in the aquifer reached 22.230°C, not exceeding the 30°C (303.15 K) threshold. However, the cold-well induced a lower minimum temperature than expected, reaching 1.95°C at the lowest, though this was not a point of concern as the cold-well had negligible influence on the system. The impact of thermal storage on the upper confining layer exists, but not significant. The average maximum temperature reached 12.55°C directly

above the warm-well and average lowest temperature above the cold-well was 11.74°C after 5 years of operation, indicating that there is slight influence of heat conducting into the confining layer due to thermal injection in the warm-well. Throughout the operation there was no significant indication of thermal interference between wells, as the temperature at the midpoint after 5 years was 0.055°C higher than ambient. The thermal plume maintained proximal to the warm-well during injection and extraction with a large temperature reduction away from the well after 15-20 m.

The ATES 30-year idle period study provided stronger understanding of how natural dispersion and conduction of stored heat works in porous media. The results from this study indicate that the thermal energy stored near the warm-well decreases at a faster rate within the first 10 years after the shut down and proceed to gradually slow as temperatures between wells and away from the warm-well approach within 2°C to 3°C above ambient. There were signs of thermal interference in layer 2 after 30 years as the temperature between wells at x = 40 m reached 12.4°C, 0.4°C above ambient, indicating the migration of the thermal front induced from the warm-well. The confining layer received a noticeable amount of heat after 30 years, specifically above the warm-well but there were elevated temperature distributions between wells that are worth mentioning. Heat added to the confining layer at the midpoint between wells reached an average temperature of 12.14°C, 0.14°C above ambient and peaked at 12.55°C directly above the warm-well after 30 years. In layer 2, the thermal plume remained rather stationary, extending no more than 20 m from the warm-well with time, however, the heat is reduced significantly over 30 years, contributing to heat gained in the confining layers.

The cold-water injection study offered key understanding how push-pull testing methods can reduce residual heat in the aquifer in both the near-term (<5 years) and long-term (>10

years). Remediation is largely controlled by injection and extraction rates compared to injection temperature, which has a much smaller influence on temperature reduction. It is determined that higher injection rates between 200-300 m^3/d within the first 1 to 5 years of push-pull testing delivered the largest impact on reducing heat in the aquifer after the shutdown of the ATES system. An injection rate of 300 m^3/d with a temperature regime of (5,5,-,5) is most effective in bringing the aquifer back to equilibrium after one year of testing, however the aquifer temperature remains 0.55°C above pre-ATES deployment conditions. After five years, a reduced flowrate of 250 m^3/d worked best as the maximum temperature reduced to 0.12°C below ambient. After 10 years, it was apparent that lower flowrates were needed to avoid over-cooling of the aquifer and therefore wasting energy and water resources. The optimal flowrates continued to decline with time as 100 m^3/d is best after 10 years, and 50 m^3/d after 15 and 20 years. Thermal energy stored near the warm-well did not remain as stationary as expected during the push-pull process. The thermal front appeared to be pushed further away from the well approximately 50 m after around 5 years as observed by the elevated temperatures closer to the cold-well which would not have occurred under natural warming. The impedance is acceptable given that this energy contributes to heating the region near the cold-well region over time, increasing the rate that the region approaches equilibrium conditions. Lastly, injection temperature regimes did not play a significant role in the thermal remediation process due to convective transport dominating conductive heat transfer.

7. FUTURE STUDIES

In the broader development of this study, it improves our ability to understand the lasting effects of thermal storage in groundwater aquifers once they've been abandoned or shutdown. This study can be extended to investigate the effects of cold-water injection on the temperature of the confining layers over time and how this influences thermal leakage back into the aquifer. Additionally, for this study there was no background flow, though for a more representative model it would be necessary to incorporate a parametrics study that investigates thermal distribution in an heterogenous aquifer given various groundwater background flowrates. This will impact thermal plume migration away from the wellbore regions, and understanding how much background flow can be achieved while maintaining optimal ATES system conditions is integral to the feasibility of the system.

Future work should acknowledge the thermal effects of these systems from a long-term hydrogeochemical perspective. For ATES to succeed, knowledge of the environmental risks related to ATES operations must be fully understood and transparent. Thermal effects from warm-water injection and thermal dispersion in the aquifer may potentially produce hydrochemical reactions due to increase temperature changes and hydraulic interference such as, mixing between stratigraphic layers, plume mobilization, oxidations/dissolutions of minerals, increasing reaction kinetics, and facilitating microbial activity (Possemiers, 2014). Long-term studies concerning the understanding of chemical changes to groundwater connected with these systems need to be developed under similar time constraints and injection/extraction principles. What are the existing geochemical conditions of the aquifer after 5, 10, 20+ years of ATES operation and how do remedial methods impact this groundwater chemistry through time?

Understanding various groundwater geochemical compositions and the role that induced temperature increases and mixing mechanisms have on disrupting or accelerating reaction kinetics due to ATES systems remains unclear. The goal is to develop reasonable understanding of how a specific aquifer's groundwater quality may be affected by these open-loop thermal storage systems before they are implemented.

ATES growth is largely controlled by social and economic barriers as well as environmental regulations that aim to not only to reduce system capital costs but also the risk of environmental issues that may arise while the technology is in operation. Gaining community social acceptance and State and National government approvals will provide the pathway for ATES systems to populate in favored hydrogeologic areas. Effective legislative frameworks that aim to provide a balance between ensuring safe groundwater drinking water, aquifer protection, and ATES technology efficiencies are still in development and are worthy of looking into in order to offer the expansion of these systems sustainably.

REFERENCES

Fleuchaus, P., 2020. Global application, performance, and risk analysis of Aquifer Thermal Energy Storage (ATES). Karlsruher Instituts für Technologie.

Ganguly, S., Mohan Kumar, M.S., Date, A., Akbarzadeh, A., 2017. Numerical investigation of temperature distribution and thermal performance while charging-discharging thermal energy in aquifer, Applied Thermal Engineering, Volume 115, Pages 756-773, ISSN 1359-4311, https://doi.org/10.1016/j.applthermaleng.2017.01.009.

Hecht-Méndez, J., Molina Giraldo, N., Blum, P., Bayer, P., 2009. Use of MT3DMS for heat transport simulation of shallow geothermal systems. AGU Fall Meeting Abstracts.

Kim, J., Lee, Y., Yoon, W.S., Jeon, J.S., Koo, M.H., Keehm, Y., 2010. Numerical modeling of aquifer thermal storage system, Energy 35:4955–4965.

Lee, KS., 2008. Performance of open borehole thermal energy storage system under cyclic flow regime. Geosciences Journal, 12(2):169e75.

Li, K.Y., Yang, S.Y., Yeh, H.D., 2010b. An analytical solution for describing the transient temperature distribution in an aquifer thermal energy storage system. Hydrological Processes 24:3676–3688.

Meng, B., Yang, Y., Huang, Y., Kolditz, O., Shao, H., 2021. Remediation Potential of Borehole Thermal Energy Storage for Chlorinated Hydrocarbon Plumes: Numerical Modeling in a Variably-Saturated Aquifer. Front. Earth Sci. 9:790315. doi: 10.3389/feart.2021.790315.

Ocłoń P. (2021) Storage of Thermal Energy in the Ground. In: Renewable Energy Utilization Using Underground Energy Systems. Lecture Notes in Energy, vol 84. Springer, Cham. https://doi.org/10.1007/978-3-030-75228-6_2.

Possemiers, M., Huysmans, M., Batelaan, O., 2014. Influence of Aquifer Thermal Energy Storage on groundwater quality: A review illustrated by seven case studies from Belgium. Journal of Hydrology: Regional Studies. 20-34.

Stopa, J., Wojnarowski, P., 2006. Analytical model of cold-water front movement in a geothermal reservoir. Geothermics 35:59–69.

Waterloo Hydrogeologic. Visual MODFLOW Flex 8.0 Help, MT3DMS/RT3D.

Yang, YS., Yeh, HD., 2008. An analytical solution for modeling thermal energy transfer in a confined aquifer system. Hydrogeology Journal 16:1507–1515.

Zheng, C., Wang, P.P., 1999. MT3DMS: A modular three- dimensional multi-species model for simulation of advection, dispersion, and chemical reactions of contaminants in groundwater systems; documentation and user's Guide, Contract Report SERDP-99-1.

APPENDIX A

Table 2.1 Physical, fluid, and thermal parameters of fluid and unconsolidated alluvial aquifer properties for modeling.

Parameter	Symbol	Unit	Value (Fine Sand)	Value (Clay)
Horizontal hydraulic conductivity	$K_x = K_y$	m day^{-1}	5	0.005
Vertical hydraulic conductivity	K_z	m day^{-1}	0.5	0.0005
Porosity of aquifer (eff)	f_a		0.25	
Porosity of overlying layer (eff)	f_1			0.15
Porosity of underlying layer (eff)	f_2			0.15
Specific storage	S_s	m^{-1}	$4.5\ 10^{-6}$	$4.5\ 10^{-5}$
Storativity	S		$4.0\ 10^{-4}$	$4.0\ 10^{-3}$
Density of fluid	r_w	kg m^{-3}	998	
Average density of aquifer	r	kg m^{-3}	2237	2487.5
Density of solids/minerals	r_b	kg m^{-3}	2650 (quartz)	2750 (illite)
Specific heat of water	c_w	J kg^{-1} K^{-1}	4189	
Specific heat of aquifer	c	J kg^{-1} K^{-1}	1000	
Specific heat of overlying layer	c_{r1}	J kg^{-1} K^{-1}		920
Specific heat of underlying layer	c_{r2}	J kg^{-1} K^{-1}		920
Volumetric heat capacity of water	C_w	J m^{-3} K^{-1}	$4.18\ 10^6$	
Volumetric heat capacity of aquifer	C_a	J m^{-3} K^{-1}	$1.85\ 10^6$	
Volumetric heat capacity of over.	C_1	J m^{-3} K^{-1}		$1.61\ 10^6$
Volumetric heat capacity of under.	C_2.	J m^{-3} K^{-1}		$1.61\ 10^6$
Thermal conductivity of aquifer (lon.)	l_{mx}	W m^{-1} K^{-1}	2.4	
Thermal conductivity of aquifer (lat.)	l_{my}	W m^{-1} K^{-1}	2.4	
Thermal conductivity of aquifer (vert.)	l_{mz}	W m^{-1} K^{-1}	0.9	
Thermal conductivity of water	l_w	W m^{-1} K^{-1}	0.6	
Thermal conductivity of overlying.	l_{r1}	W m^{-1} K^{-1}		1.8
Thermal conductivity of underlying	l_{r2}	W m^{-1} K^{-1}		1.8
Distribution coefficient	K_d	m^3 kg^{-1}	$2.125\ 10^{-4}$	$2.068\ 10^{-4}$
Longitudinal dispersivity	a_L	m	0.5	0.05
Thermal diffusivity	D_{th}	m^2 d^{-1}	0.198	0.10
Retardation factor	R		2.90	
Darcy Velocity	q_0	m d^{-1}	0.00	0.00
Initial temperature of aquifer	T_{A01}	K	285.15	
Initial temperature of overlying layer	T_{01}	K		285.15
Initial temperature of underlying layer	T_{02}	K		285.15
Thickness of aquifer	B	m	50	
Thickness of overlying layer	b_1	m		30
Thickness of underlying layer	b_2	m		30

Values obtained from (Kim et. al., 2010), (K.S. Lee, 2008), (Hecht-Méndez, 2010), and (Ganguly and Kumar, 2017).

APPENDIX B

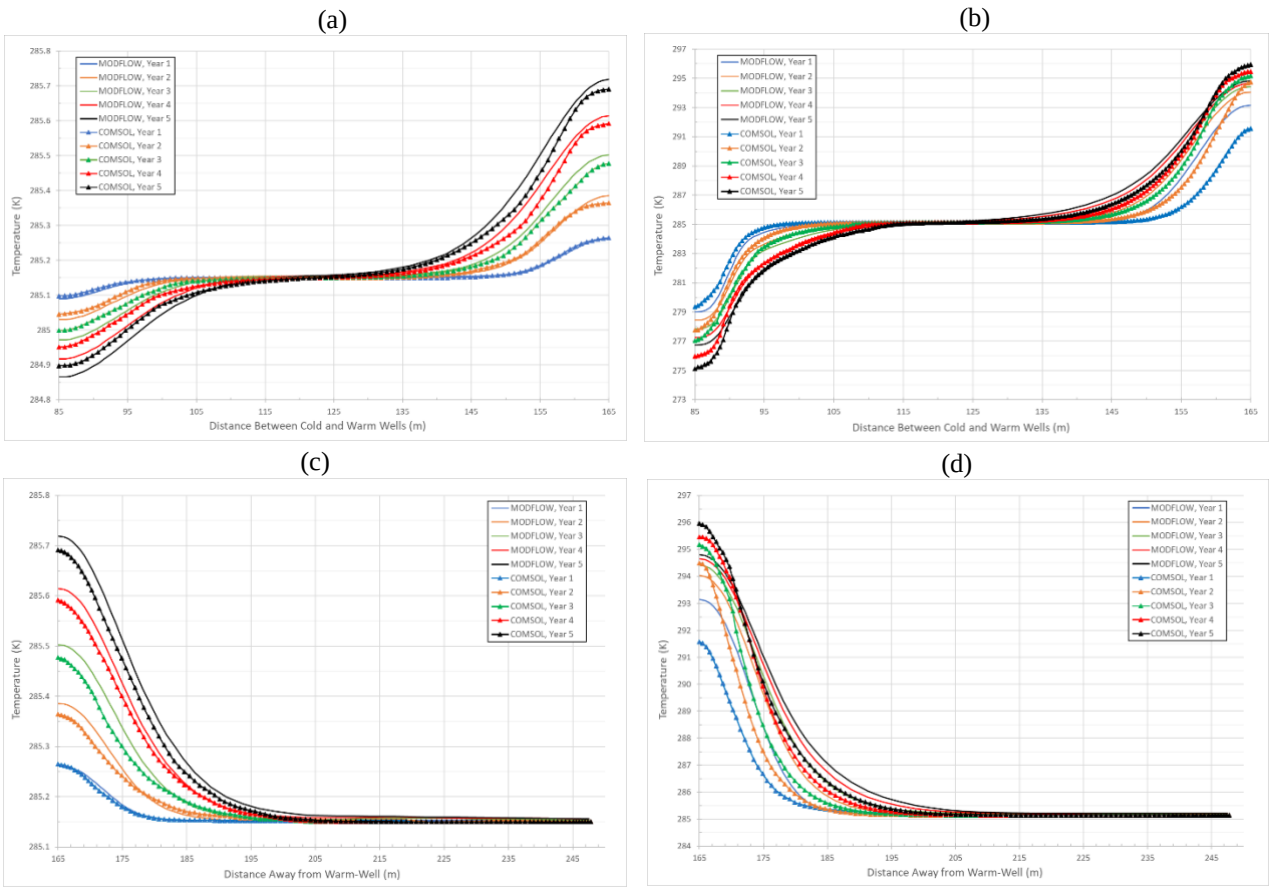

Figure 5.2. Comparison between MODFLOW and COMSOL temperature distributions with radial distance due to thermal injection and extraction over a five-year period for (a) case between wells in layer 1, (b) case between wells in layer 2, (c) case away from warm-well in layer 1, and (d) case away from warm-well in layer 2.

(e)

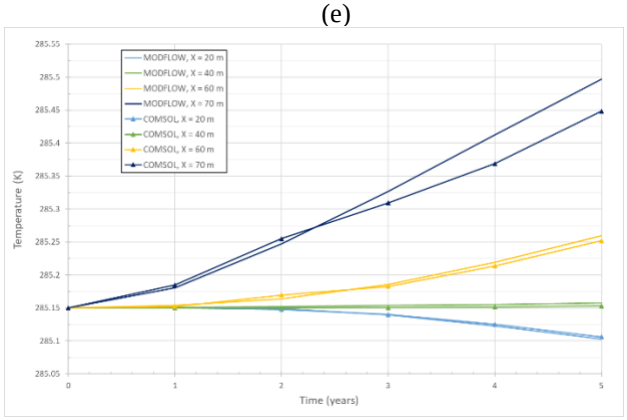

(f)

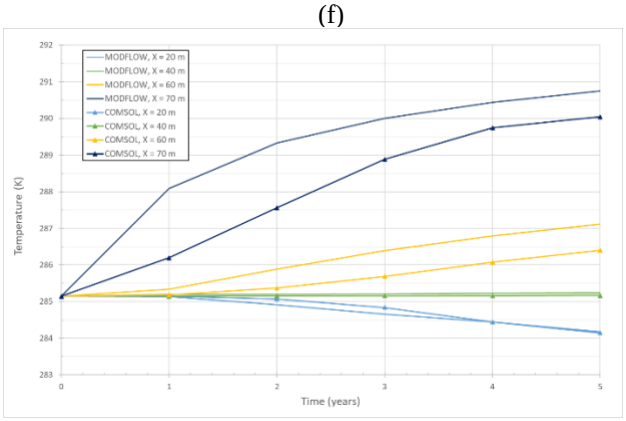

(g)

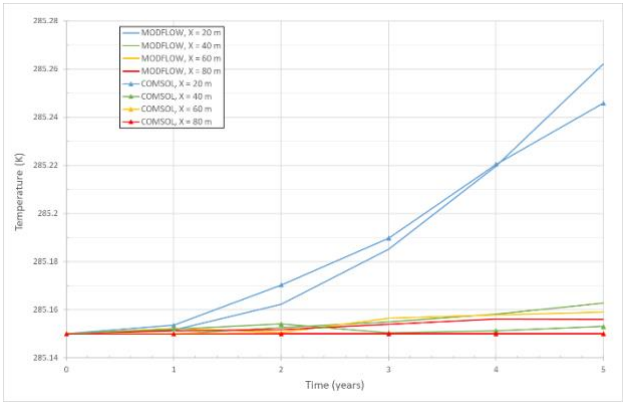

(h)

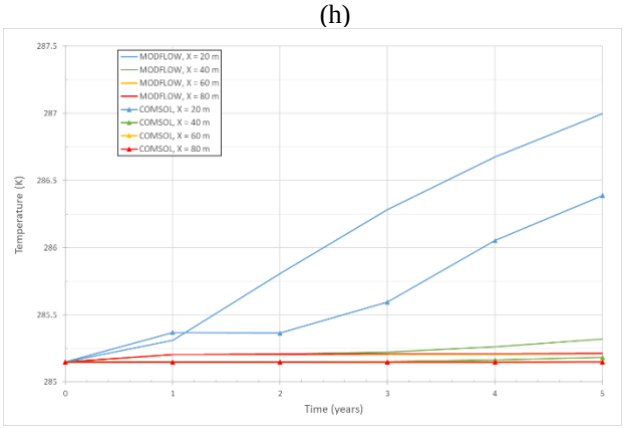

Figure 5.2.1 Comparison between MODFLOW and COMSOL temperature distributions with time due to thermal injection and extraction over a five-year period for (e) case between wells in layer 1, (f) case between wells in layer 2, (g) case away from warm-well in layer 1, and (h) case away from warm-well in layer 2.

APPENDIX C

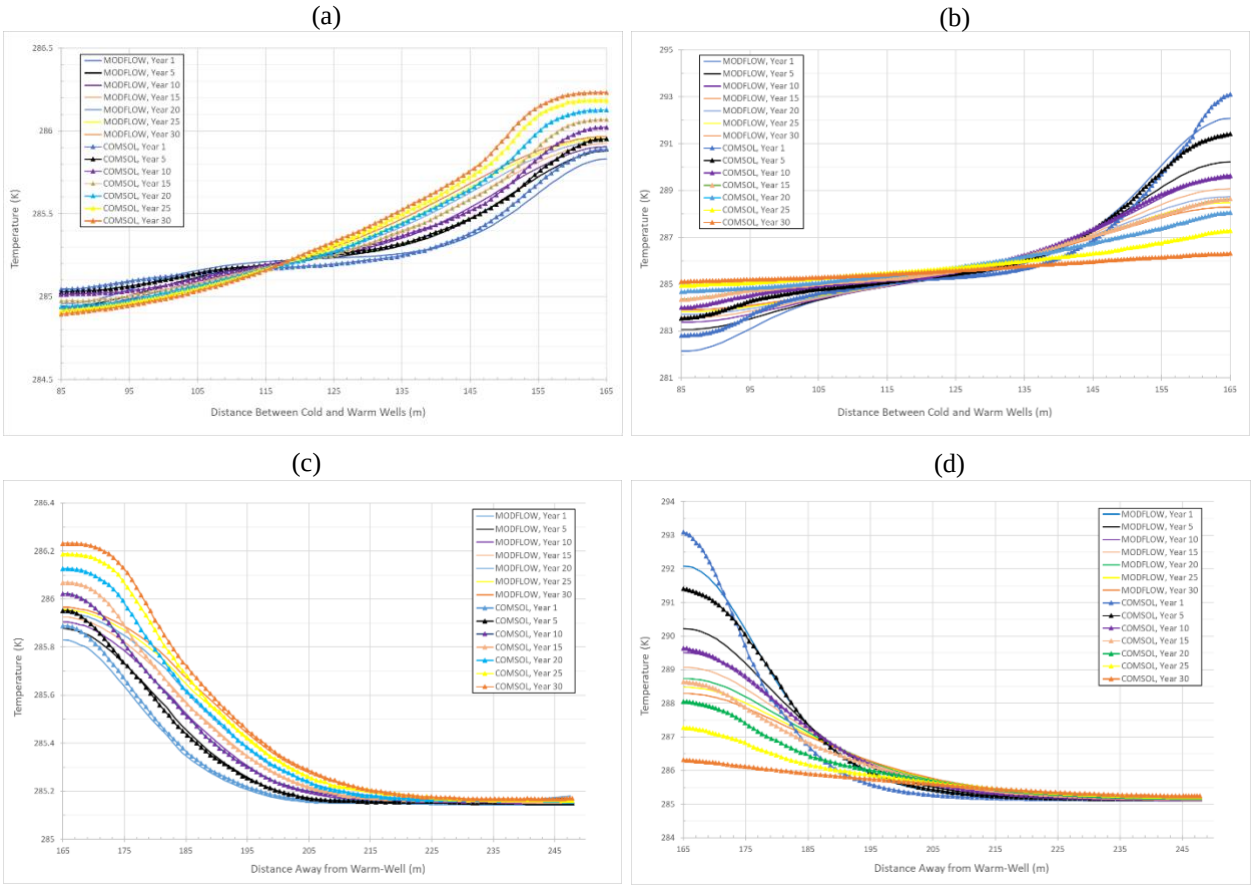

Figure 5.3. Comparison between MODFLOW and COMSOL temperature distributions with radial distance when wells are shut down the system is in idle for 30-years for (a) case between wells in layer 1, (b) case between wells in layer 2, (c) case away from warm-well in layer 1, and (d) case away from warm-well in layer 2.

(e)

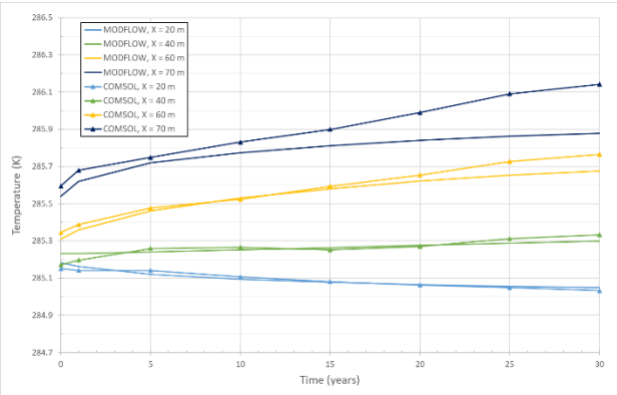

(f)

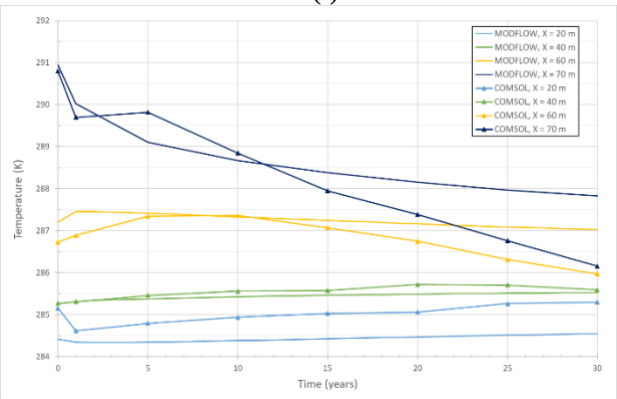

(g)

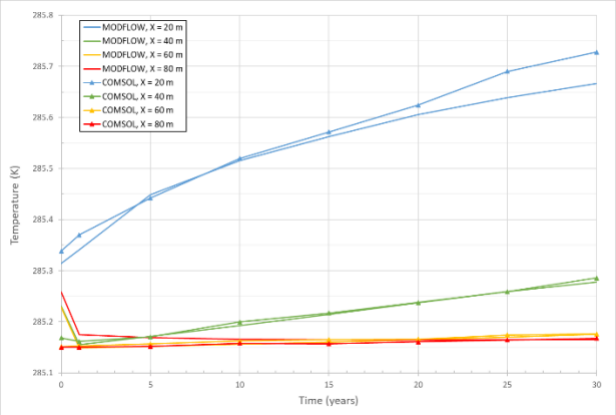

(h)

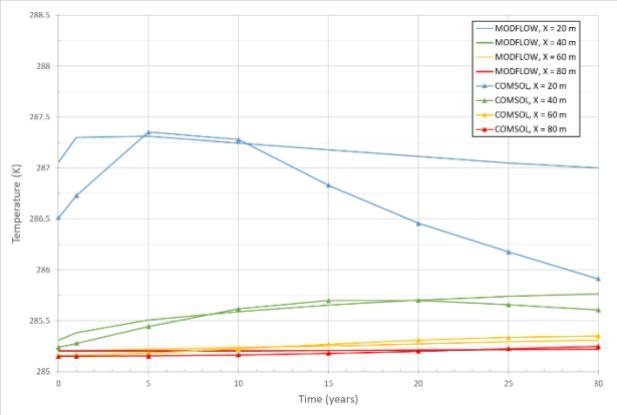

Figure 5.3.1 Comparison between MODFLOW and COMSOL temperature distributions with time due to the shut-down of the wells during the 30-year idle for (e) case between wells in layer 1, (f) case between wells in layer 2, (g) case away from warm-well in layer 1, and (h) case away from warm-well in layer 2.

APPENDIX D

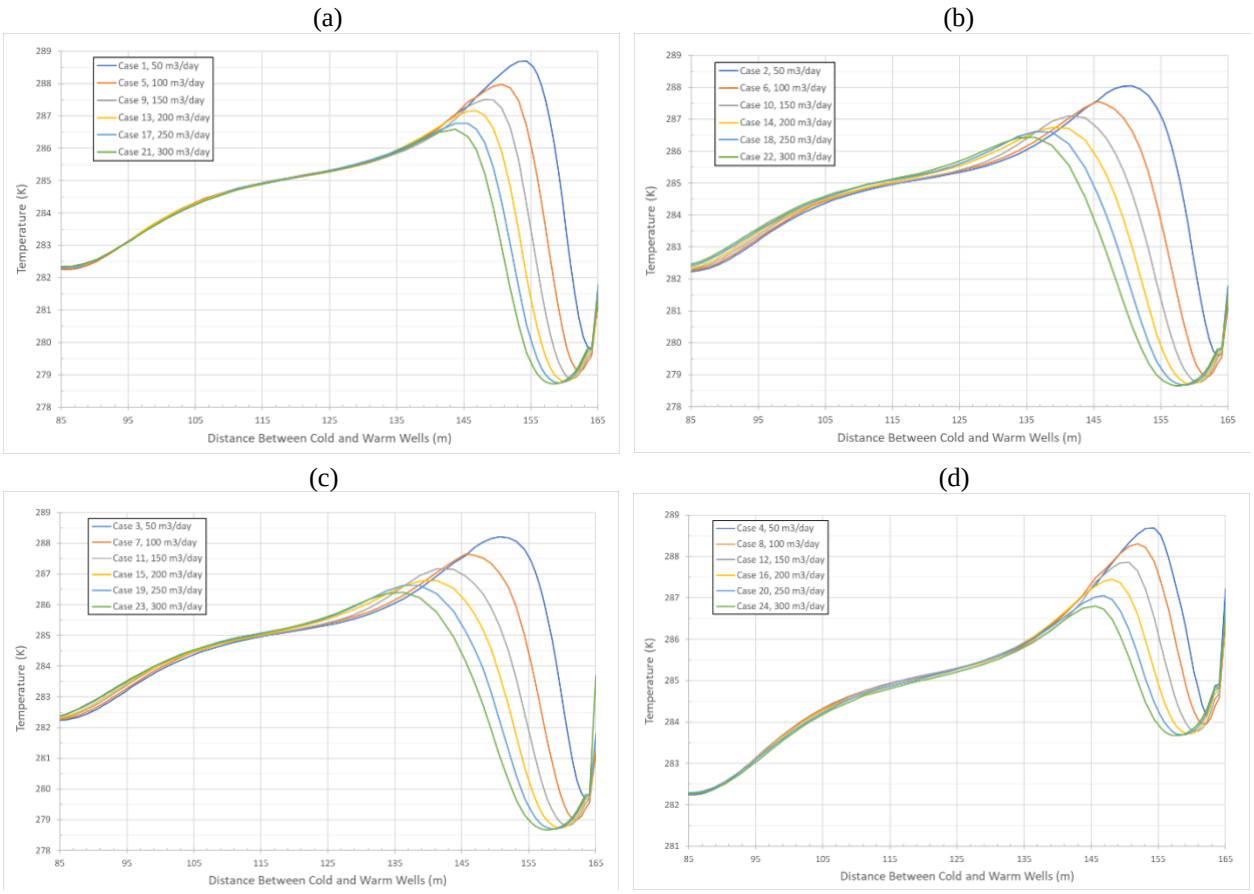

Figure 5.4 Comparison between MODFLOW temperature distributions with radial distance due to cold-water injection and extraction in layer 2 at variable rates after one year for (a) case of (5,-,-,5) regime (b) case of (5,5,-,5) regime, (c) case of (5,10,-,5) regime, and (d) case of (10,-,-,10), based on injection temperature variability given in Table 4.3.

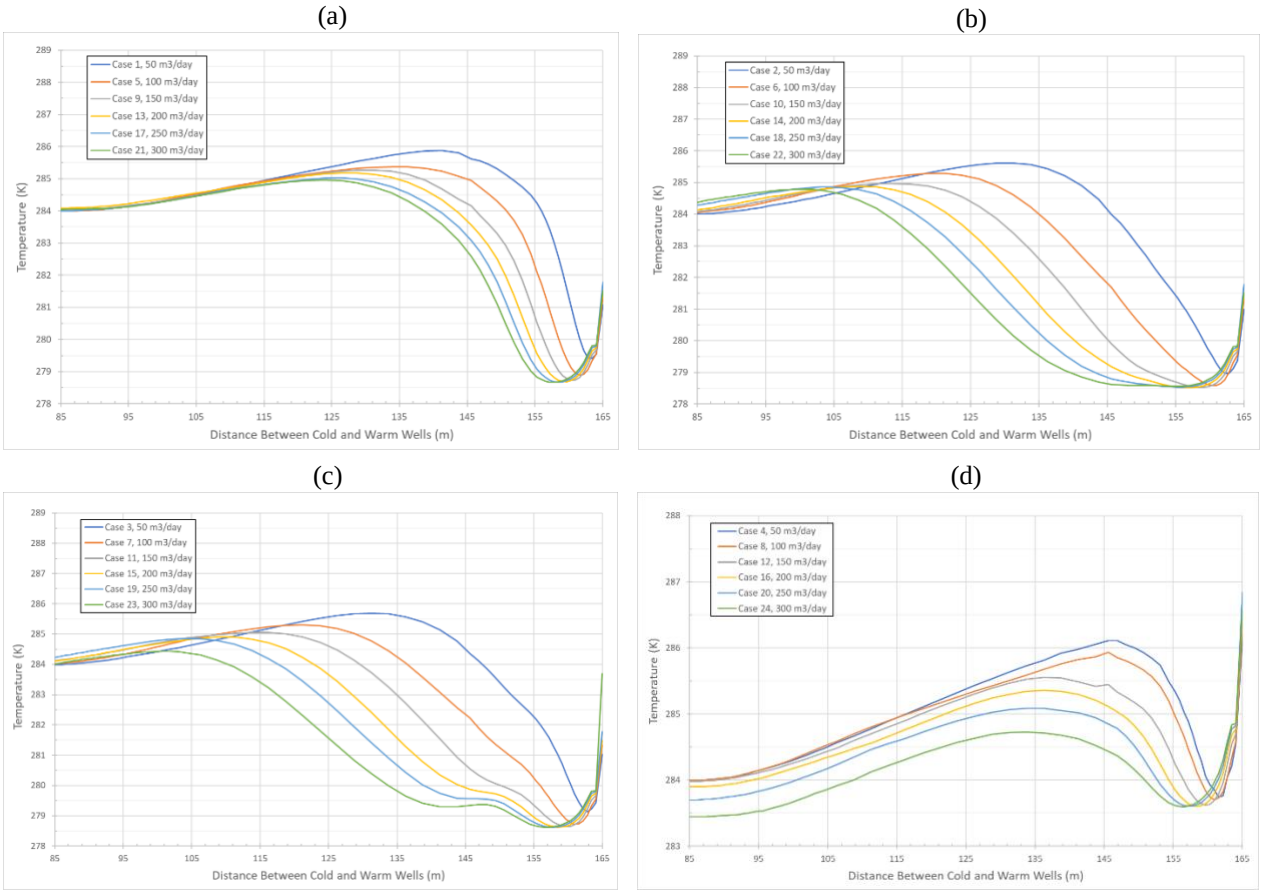

Figure 5.4.1 Comparison between MODFLOW temperature distributions with radial distance due to cold-water injection and extraction in layer 2 at variable rates after five years for (a) case of (5,-,-,5) regime (b) case of (5,5,-,5) regime, (c) case of (5,10,-,5) regime, and (d) case of (10,-,-,10), based on injection temperature variability given in Table 4.3.

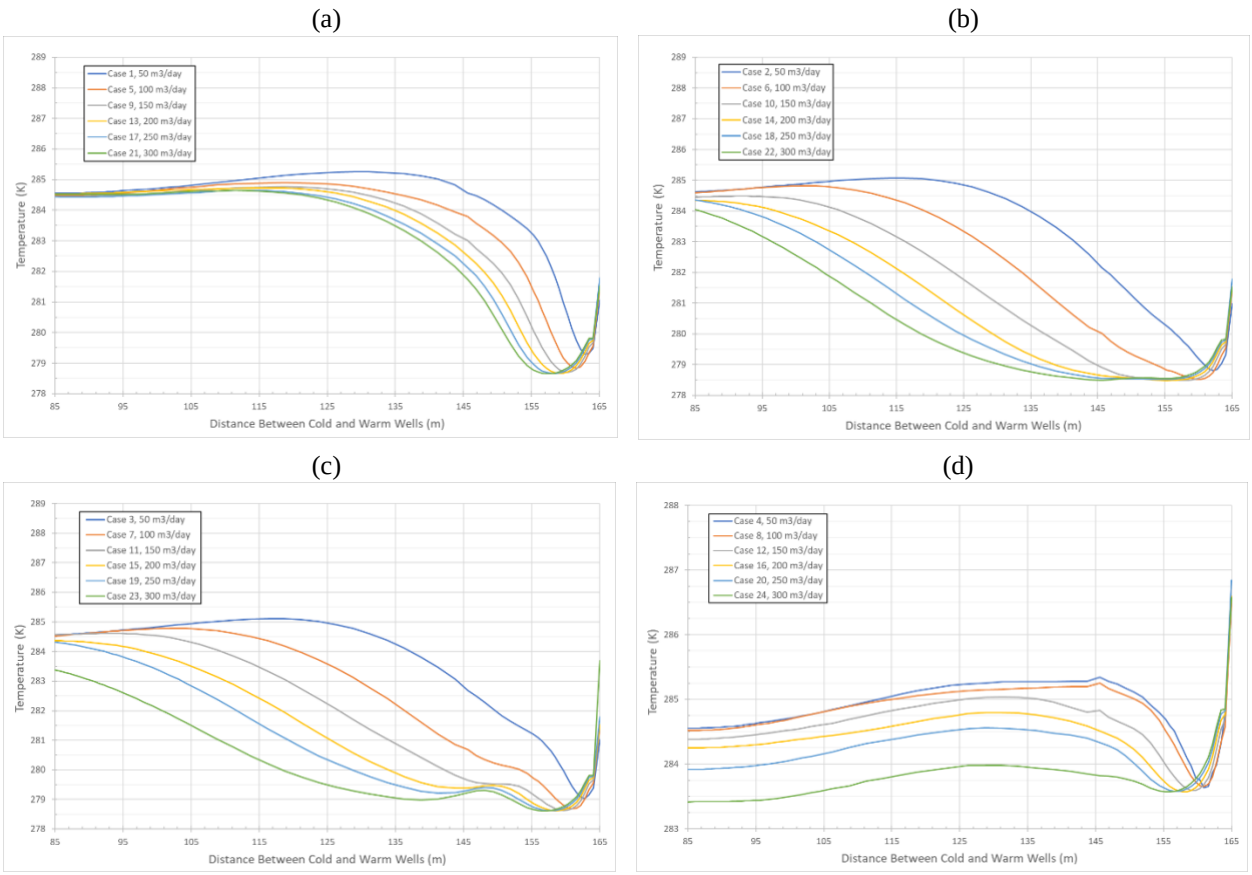

Figure 5.4.2 Comparison between MODFLOW temperature distributions with radial distance due to cold-water injection and extraction in layer 2 at variable rates after 10 years for (a) case of (5,-,-,5) regime (b) case of (5,5,-,5) regime, (c) case of (5,10,-,5) regime, and (d) case of (10,-,-,10), based on injection temperature variability given in Table 4.3.

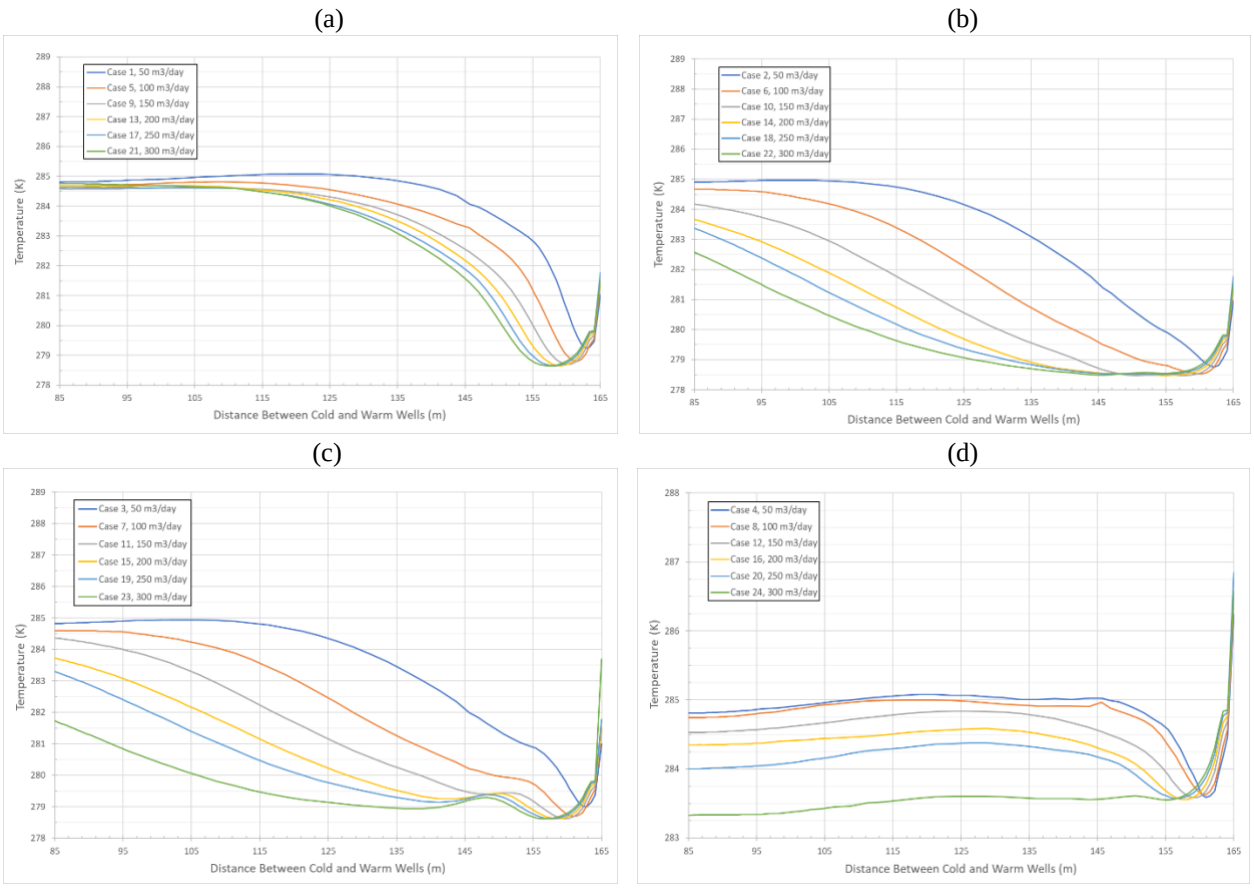

Figure 5.4.3 Comparison between MODFLOW temperature distributions with radial distance due to cold-water injection and extraction in layer 2 at variable rates after 15 years for (a) case of (5,-,-,5) regime (b) case of (5,5,-,5) regime, (c) case of (5,10,-,5) regime, and (d) case of (10,-,-,10), based on injection temperature variability given in Table 4.3.

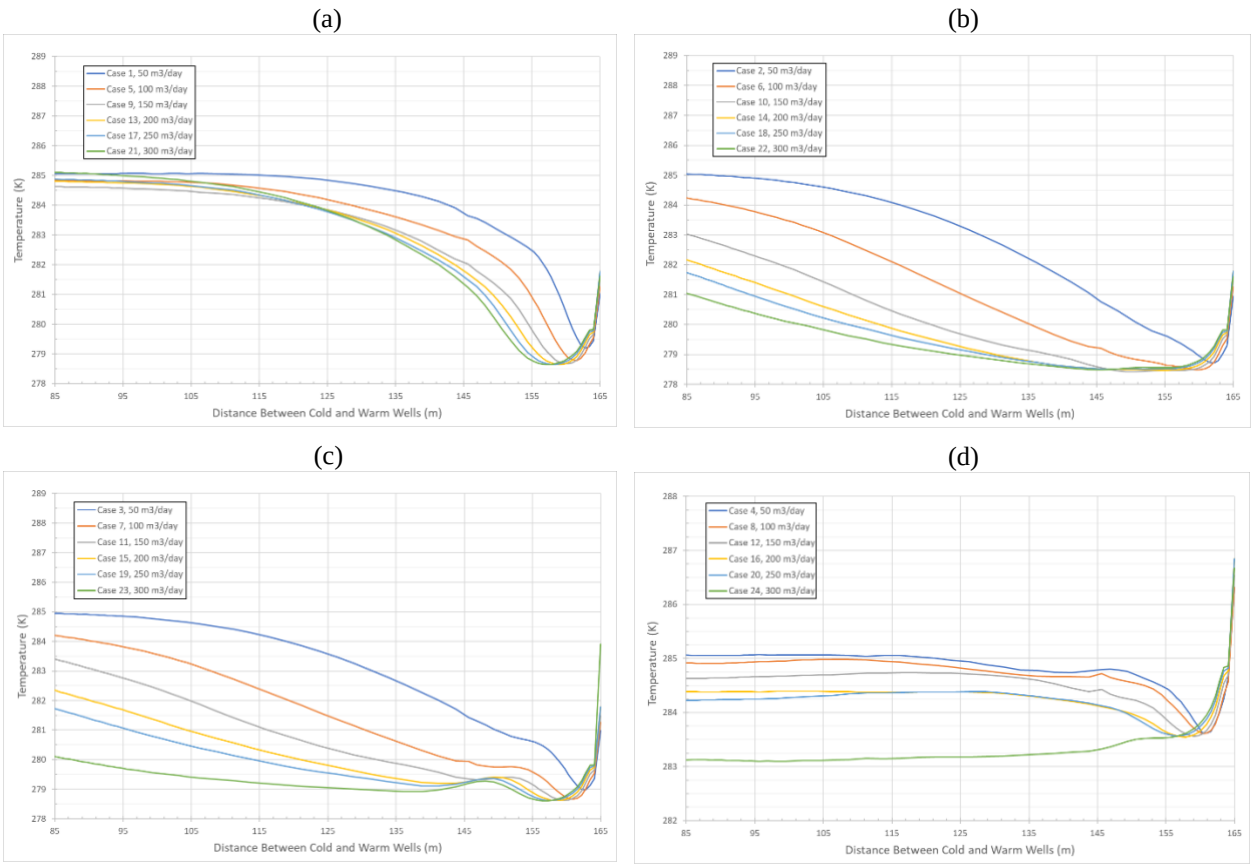

Figure 5.4.4 Comparison between MODFLOW temperature distributions with radial distance due to cold-water injection and extraction in layer 2 at variable rates after 25 years for (a) case of (5,-,-,5) regime (b) case of (5,5,-,5) regime, (c) case of (5,10,-,5) regime, and (d) case of (10,-,-,10), based on injection temperature variability given in Table 4.3.